



HEAT CONVECTION WITH PHASE CHANGE

Heat convection with phase change	1
Boiling.....	2
Pool boiling.....	3
Nucleate boiling	3
Flow boiling	5
Condensation.....	6
Natural film condensation.....	7
Forced flow condensation	10
Two-phase loops	10
Heat pipes.....	11
History and applications.....	13
Operations overview	15
Design and operating limits	19
Thermodynamic processes in a LHP	21
Flow inside the wick	23
Boiling inside the wick	28
Evaporative cooling	29
Evaporation in a pool of water.....	29
Cooling towers	33

HEAT CONVECTION WITH PHASE CHANGE

We have studied [heat convection without phase change](#) aside, i.e. the influence of fluid flow (either imposed or naturally created) on heat conduction at a washed wall. A [phase change](#) in a substance may occur without heat transfer (e.g. in an adiabatic flash chamber, or by heavy isothermal compression of an ice cube, or by stirring a water-ice bath in an adiabatic calorimeter).

Here we want to analyse the effect of phase changes in heat convection, particularly in the case of phase changes between fluid phases (liquid to gas or gas to liquid), leaving convection with solid phase change aside (though the problem of freezing in pipe flow has been much studied, e.g. by Weigand B, Braun J, Neumann SO, Rinck KJ, “Freezing in forced convection flows inside ducts: A review”. Heat Mass Transf. 32:341-351, 1997). Conduction with phase change, basically reduces to the classical [Stefan problem](#) of [freezing and thawing \(presented in Heat Conduction\)](#); see also [Exercise 11, in Heat Transfer](#).

The involved enthalpy and density changes in phase transition, render the problem difficult to model and solve. Recall that fluid phase transitions can only occur below the [critical point for the fluid](#) (e.g. liquid water at $p > 22$ MPa cannot be made to boil at any temperature (but reducing the pressure may do it), and water vapour at $T > 650$ K cannot be made to condense at any pressure, although reducing the temperature may do it). Further notice that the same phase-change in a pure substance (liquid to vapour, or vapour to liquid) can be achieved without boiling or condensation within the heat exchanger (e.g. by heating a

pressurized liquid and subsequent flashing), but heat transfer with phase change is much more efficient (less required area).

Convective problems with phase change may be grouped in different ways:

- By type of phase change, i.e. from liquid to gas, or from gas to liquid (excluding solid changes).
- By type of convection initiation, i.e. forced, or natural convection.
- By type of fluid composition, i.e. phase-change in pure substances (e.g. from water to steam), or in mixtures. A special case of the latter is when only one component of the mixture changes phase (e.g. from humid air to a mist).

The analysis that follows here focus on four main topics:

- Boiling, i.e. liquid-to-vapour change, mainly in a pure substance.
- Condensation, i.e. vapour-to-liquid change, mainly in a pure substance.
- Two-phase loops, i.e. a liquid-to-vapour-to-liquid change as used in some demanding steady-state heat convection applications like heat pipes.
- Evaporative cooling, i.e. evaporation of a liquid (or some component of a liquid mixture) in a non-saturated gas atmosphere.

BOILING

Boiling, or vaporising, is the transition from a liquid phase to its vapour phase at the liquid-vapour-equilibrium temperature (to distinguish it from evaporation, which takes place at lower temperatures in a gas mixture). Mind, however, that evaporation is often used as a synonym of vaporisation, especially in refrigeration equipment, where the heat exchanger where the refrigerant boils (most of the times a pure substance) is named 'evaporator' almost universally.

Boiling usually takes place at solid surfaces heated above the boiling temperature, although it may take place in the bulk by lowering pressure until liquid-vapour equilibrium (e.g. in a flash chamber). Initial bubble formation is trade-off process known as nucleation (see [Vaporization kinetics](#)), because only relatively-large bubbles can grow (very small bubbles tend to collapse by surface tension); the most common bubble formation process is by heterogeneous nucleation, i.e. bubbles growing on already-existing surface crevices of solid particles in the bulk. That is why minute changes in surface cleaning or liquid solutes may have a profound influence on the start of boiling (but boiling heat transfer usually focuses on the steady state and not on the onset of boiling).

Two basic boiling configurations can be distinguished: pool boiling (or natural convection boiling, i.e. boiling in an otherwise quiescent liquid mass), and flow boiling (or forced convection boiling, boiling inside tubes).

The large density difference between the liquid and vapour phases makes boiling (and condensation) heavily dependent on the presence and orientation of force fields like gravity (or centrifugation). Of particular importance is the [boiling under microgravity](#) (particularly on pool boiling).

Vaporisation in porous media is a very efficient heat transfer method used in heat pipes, capillary pumped loops, and loop heat pipes.

Pool boiling

The simplest case of boiling is that induced by a heated horizontal wire within a liquid pool open to the atmosphere (if it were closed, some special buffer space would be needed to avoid a pressure surge).

If we concentrate on the common case of boiling water at normal pressure in air, not heated from the bottom as usual, but with a thin horizontal platinum wire as the only heater in the bulk, we may observe different boiling regimes, plotted in Fig. 1 (first described by Nukiyama in 1934), depending on the temperature of the wire surface, T_s (really the difference between that and the saturation or boiling temperature, i.e. on $T_s - T_b$).

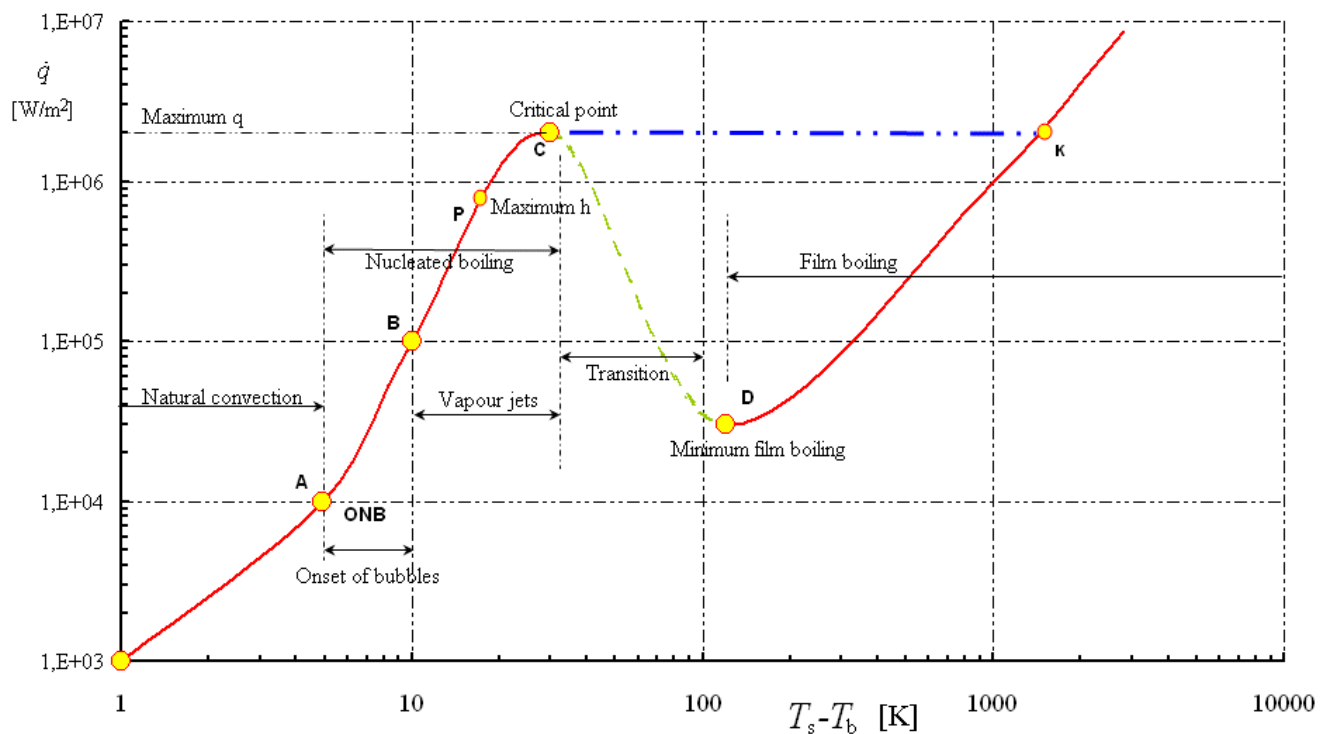


Fig. 1. Pool boiling regimes (values applicable to water).

For a wire temperature increasing from that of the liquid water, $T_s \leq T_b$, up to 105 °C (i.e. up to $T_s - T_b = 5$ K; from origin to point A in Fig. 1), no boiling occurs, in spite of equilibrium boiling being at $T_b = 100$ °C; a homogeneous natural convection is just established, at an increasing pace with wire temperature (with the evaporation rate at the free surface increasing too). Thus, the correlation for natural convection around a horizontal cylinder with laminar flow, $Nu_D = 0.53Ra_D^{1/4}$, can be applied up to point A.

Nucleate boiling

From 105 °C to 130 °C (A to C in Fig. 1), bubbles start to form over the wire and get detached as a rising bubble-stream (nucleate boiling) that collapse before reaching the free surface, getting a peak-maximum of heat flux above 1 MW/m² at a so-called critical point (or CHF, critical heat flux)..

A correlation for this peak-flux value was developed by N. Zuber in 1958, valid for cylindrical or planar horizontal heaters:

$$\dot{q}_{\max} = 0.15 \rho_V h_{LV} \left(\frac{(\rho_L - \rho_V) \sigma g}{\rho_V^2} \right)^{\frac{1}{4}} \quad (1)$$

where σ is the surface tension value at boiling temperature (like for the other values). Typical values of the heat-convection coefficient are in the range $h = \dot{q}/\Delta T = 10^3 \dots 10^4 \text{ W}/(\text{m}^2 \cdot \text{K})$.

The vertical temperature-profile would show a fluctuating slope from the wire to a nearby accommodation to the saturation temperature in the rest of the liquid; meanwhile, the vaporisation would have swept other gases from the air at the free surface, and a pure vapour phase would have been established over the liquid.

If the heating power of the wire is increased beyond that critical point (C in Fig. 1), the wire temperature suddenly jumps from some 130 °C to some 1500 °C (C to K in Fig. 1), a surge that would burn the wire if iron or copper had been used instead of platinum. If we then decrease the heating power supplied, a hysteric cycle shows up, with the wire temperature smoothly decreasing from 1500 °C to 210 °C (K to D in Fig. 1), the wire being surrounded by a vapour layer (film-vapour boiling), and then suddenly receding to the nucleate boiling regime at some 107 °C.

Notice how important it may be not to exceed the maximum heat-rate (critical point, C in Fig. 1); e.g. in a boiling water nuclear reactor (BWR), it would cause an overheating of the nuclear-rod cladding, followed by mechanical failure and release of fission products.

The local minimum of the heat flux, named [Leidenfrost](#) point in honour of this 18th c. German doctor (who described the falling of water drops over very-hot plates), has been correlated as:

$$\dot{q}_{\min} = 0.09 \rho_V h_{LV} \left(\frac{(\rho_L - \rho_V) \sigma g}{\rho_L^2} \right)^{\frac{1}{4}} \quad (2)$$

The actual details in pool boiling depend on several features: on the initial liquid temperature (e.g. if it is undercooled, bubbles collapse before reaching the free surface), on liquid-solid wetting conditions, on impurities (they increase the number of nucleation sites), etc.

When pool boiling is due to heating the liquid by heat transfer through a bottom plate, instead of the temperature surge mentioned above, when the critical point C in Fig. 1 is reached, the surge is in thermal resistance due to the vapour film, with a smooth temperature increase of the plate while heat flux decreases (transition regime in Fig. 1), until around 210 °C the whole plate becomes dry (covered by a vapour layer; C to D in Fig. 1).

When boiling takes place at vertical walls (wall heating) in a pool, the process resembles more flow boiling at low speed than pool boiling.

Nucleate boiling of azeotropic mixtures is similar to that of pure liquids, but when there is segregation in the phase change (zeotropic boiling), the associated mass transfer tends to reduce the heat transfer coefficient.

Flow boiling

Relative to pool boiling, heat transfer is enhanced when there is a forced relative motion between the heater and the fluid, more pronounced in the homogeneous convection zone (left region in Fig. 1, that now changes from natural to forced convection), than in peak values (e.g. the peak heat flux measured in water increasing from 1.3 MW/m² to a maximum of 35 MW/m²). Internal flow boiling presents more variations, since it is a complicated two-phase flow.

The most-important configurations of flow boiling are: the vertical pipe, the horizontal pipe, and the micro-channels (e.g. for plate heat exchangers). In the former and commonest case, a liquid is slowly forced upwards (say at several centimetres per second, since the phase change multiplies the speed 100 to 1000 times, and choking must be prevented), inside a pipe (of internal diameter in the range 5..50 mm) with a hot wall surface at $T_s > T_{sat}(p)$, and the transition from liquid to vapour develops along several intermediate stages of two-phase-flow, from single-phase liquid to single-phase vapour, as shown in Fig. 2: bubbly zone, slug zone, churn zone, annular zone, and droplet flow, with the heat flux having a pronounced maximum in the annular region.

Vapour bubbles start forming at the superheated wall after the onset of nucleate boiling, getting detached by shear and buoyancy forces, migrating towards the axis, and collapsing within the colder compressed liquid core (bubbly flow). When the liquid core has been heated up to saturation, bubbles no longer collapse but coalesce in large voids (slug flow), pushing most of the remaining liquid against the walls (annular flow of a liquid film with a misted core), and leaving some droplets entrained until complete vaporisation.

Figure 3 gives some details of flow boiling within horizontal pipes. In all cases of multiphase flow the velocities of the phases are usually not equal), whereas in the case of adiabatic wall (with boiling due to the pressure loss), the flow structure changes only longitudinally.

Many empirical correlations can be found in the literature, but its actual applications have great uncertainties due to the high sensitivity of heat transfer to minute details in the actual configuration (e.g. fluid impurities, wall finishing, and so on). Typical values of the heat-convection coefficient are in the range $h = \dot{q}/\Delta T = 10^4 \dots 10^5 \text{ W}/(\text{m}^2 \cdot \text{K})$.

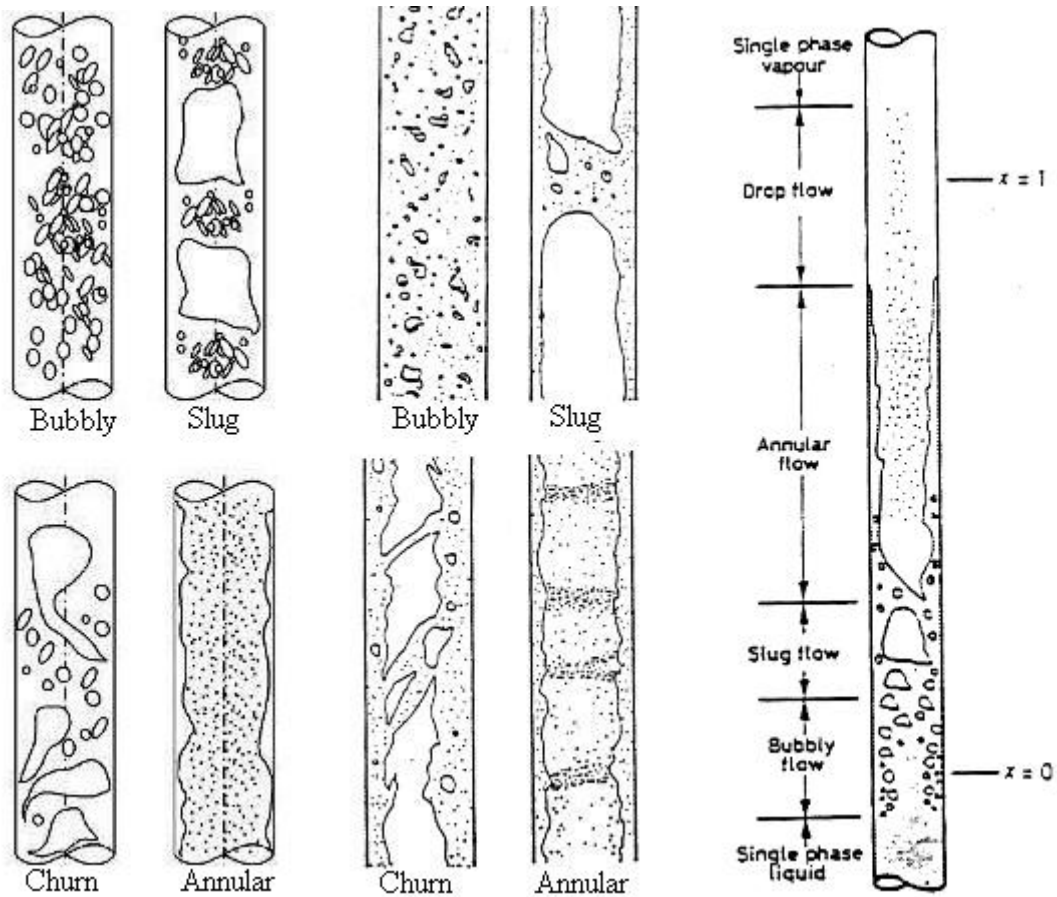


Fig. 2. Different regimes in adiabatic flow vertical upwards inside a pipe (boiling due to pressure loss), and, in the left, its development for diabatic flow (boiling due to heating through the pipe wall). From Taitel et al. (1980).

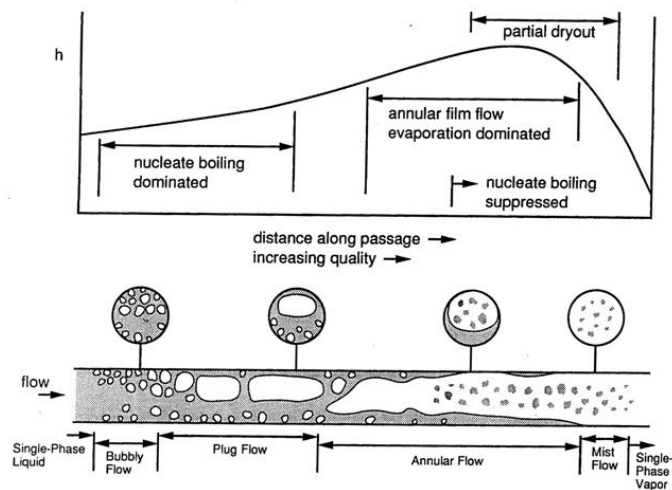


Fig. 3. Heat convection coefficient, h , and regime types, in horizontal flow boiling in a moderately superheated pipe (Kreith, 2000).

CONDENSATION

Condensation is the transition from a gas phase to a condensed phase (here, to a liquid phase; condensation to solid phase is usually called frosting, in the case of water vapour; or vapour deposition, in general).

The condensation of vapours from a pure substance on a cold solid wall may occur in droplet form (i.e. as isolated droplets like dew on leaves, which run down inclined surfaces forming rivulets and ultimately falling down), or in film form (i.e. as a continuous liquid layer). Droplet condensation is more efficient (up to ten times higher heat-transfer rates), but, although initial operation usually produce droplet condensation, there is a universal tendency to film condensation after prolonged operation; applying non-wetting coatings retards the transition, but it finally takes place anyway. Moreover, film condensation is more amenable to analytical modelling, particularly for vertical plates in natural convection, thus, we just focus on that.

Natural film condensation

Let us consider a semi-infinite vertical plate at temperature T_w within a medium composed of a pure-substance vapour (so no segregation occurs), at $T_\infty > T_w$, with the saturation temperature in between: $T_w < T_{sat} < T_\infty$. In the steady state, a two-dimensional liquid film of width $\delta(x)$ will develop, as sketched in Fig. 4 (notice the special choice of coordinates, to have x as longitudinal coordinate).

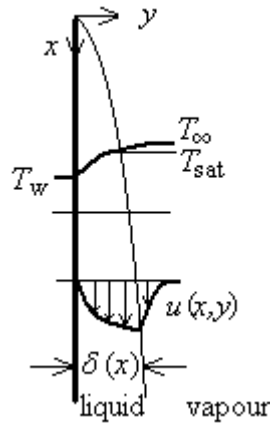


Fig. 4. Film condensation on a cold vertical plate.

The balance equations applied within the liquid boundary layer (incompressible model) are:

- Mass balance (continuity):

$$\nabla \cdot \vec{v} = 0 \quad \rightarrow \quad \frac{\partial u}{\partial x} + \frac{\partial v}{\partial y} = 0 \quad \rightarrow \quad \frac{u_m}{L} \approx \frac{v_m}{\delta} \quad (3)$$

where u_m and v_m are maximum or mean velocity values (here we do not have an imposed value as in [forced convection](#), u_∞), showing, as before, that the velocity field is basically one-dimensional, i.e. boundary-layer thickness, δ , much smaller than the length of the plate, L .

- Momentum balance:

$$\frac{D\vec{v}}{Dt} = -\frac{\nabla p}{\rho} + \vec{g} + \nu \nabla^2 \vec{v} \quad \rightarrow \quad u \frac{\partial u}{\partial x} + v \frac{\partial u}{\partial y} = -\frac{\rho_{vap} g}{\rho} + g + \nu \frac{\partial^2 u}{\partial y^2} \quad \rightarrow \quad g \approx \nu \frac{u_m}{\delta^2} \quad (4)$$

the latter obtained by neglecting inertia stresses against viscous stresses, and the density of the vapour phase against that of the liquid. Equation (4) relates the cause of motion (gravity) with its amount, u_m . As usual, the transverse component of the momentum balance just teaches that pressure is constant transversally.

- Energy balance:

$$\frac{DT}{Dt} = a\nabla^2 T + \frac{\phi}{\rho c_p} \rightarrow u \frac{\partial T}{\partial x} + v \frac{\partial T}{\partial y} = a \frac{\partial^2 v}{\partial y^2} \rightarrow u_m \frac{\Delta T}{L} \approx a \frac{\Delta T}{\delta_T^2} \quad (5)$$

since, again, continuity shows that the two convective terms are of the same order). Energy dissipation is negligible.

The energy balance relates the velocity generated, u_m , with the thermal thickness, δ_T , what, upon substitution in the momentum equation, with $\delta \approx \delta_T$ ($Pr \approx 1$), yields:

$$g \approx v \frac{u_m}{\delta^2} \rightarrow g \approx v \frac{aL}{\delta^2 \delta_T^2} = v \frac{aL}{\delta^4} \rightarrow \frac{\delta}{L} \approx \left(\frac{av}{gL^3} \right)^{\frac{1}{4}} \rightarrow \delta(x) \approx \left(\frac{av}{g} x \right)^{\frac{1}{4}} \quad (6)$$

This relation can be expressed in terms of the traditional Nusselt number and a Rayleigh number defined in terms of the density variation, as:

$$\left. \begin{array}{l} Nu \equiv \frac{hL}{k} = \frac{L}{\delta_T} \\ Ra \equiv \frac{\Delta\rho_{LV} gL^3}{\rho_L av} \end{array} \right\} \frac{\delta}{L} \approx \left(\frac{av}{gL^3} \right)^{\frac{1}{4}} \xrightarrow{\frac{\Delta\rho_{LV}}{\rho_L}=1, \frac{\delta}{\delta_T} \approx 1} Nu \approx Ra^{1/4} \quad (7)$$

although it is traditionally expressed in terms of a modified Rayleigh number, Ra^* , defined to include the so-called Jakob number Ja , as:

$$Ja \equiv \frac{h_{LV}}{c\Delta T}, \rightarrow Ra^* \equiv Ra Ja = \frac{\Delta\rho_{LV} gL^3}{\rho_L av} \frac{h_{LV}}{c\Delta T} = \frac{(\rho_L - \rho_V) h_{LV} gL^3}{\nu_L k_L (T_{sat} - T_w)} \quad (8)$$

where subindices have been added to make explicit reference to the phase implied. Notice that T_{sat} is the saturation temperature at the operating pressure, $T_w < T_{sat} < T_\infty$; in fact, if T_∞ and T_w differ a lot from T_{sat} , the enthalpy change should be corrected to $h'_{LV} = h_{LV} + (2/3)c_{pL}(T_{sat} - T_w) + c_{pV}(T_\infty - T_{sat})$.

The exact solution, once again integrating across the thickness of the boundary layer, was obtained in 1916 by Nusselt, namely:

$$Nu_L = 0.94(Ra_L^*)^{1/4} \quad (9)$$

which favourably compares with our estimation (7). Nusselt's solution (9) is only valid for laminar flow; it is based on the simplified analysis with a parabolic velocity profile $u(x,y)=u_m(x)(2y/\delta-(y/\delta)^2)$, see Fig. 4, and a linear temperature profile $T(x,y)=T_w+(T_{sat}-T_w)(y/\delta)$; from $\dot{q} = h_x(T_w - T_{sat}) = -k_L \partial T/\partial y|_{y=0}$ he got (see e.g. Çengel-2003):

$$\begin{aligned} \delta(x) &= \left(\frac{4\mu_L k_L (T_{sat} - T_w)}{g\rho_L(\rho_L - \rho_V) h_{LV}} x \right)^{1/4}, \quad h(x) = \left(\frac{g\rho_L(\rho_L - \rho_V) k_L^3 h_{LV}}{4\mu_L (T_{sat} - T_w)} \frac{1}{x} \right)^{1/4} \\ \Rightarrow h_L &= \int_0^L h(x) dx = \frac{4}{3} h(x)|_{x=L} = \frac{2\sqrt{2}}{3} \left(\frac{g\rho_L(\rho_L - \rho_V) k_L^3 h_{LV}}{4\mu_L (T_{sat} - T_w)} L \right)^{1/4} \\ \Rightarrow Nu_L &= \frac{h_L L}{k_L} = \frac{2\sqrt{2}}{3} (Ra_L^*)^{1/4}, \quad \frac{\delta(x)}{x} = \frac{\sqrt{2}}{(Ra_L^*)^{1/4}} \end{aligned} \quad (10)$$

Notice that a growth law $\delta(x) \propto x^{1/4}$ can also be deduced from (6), and, jointly with (4), yields $u_m \propto \delta^2 \propto x^{1/2}$; furthermore, the condensing flow-rate per unit width is $\dot{m}/b = \rho_L u_m \delta \propto x^{3/4}$; on the other hand, $\dot{m} h_{LV} = h_L L b (T_{sat} - T_w) = b k_L (T_{sat} - T_w) Nu_L$ (do not confuse subindex L for length in h_L with subindex L for liquid in k_L). In terms of a Reynolds number, defined by $Re_{\delta}(x) \equiv 4u_m \delta(x)/\nu$ (the 4 is for the equivalent hydraulic diameter of the falling film, $D_h=4\delta$), the flow starts to wave at $Re_{\delta} > 30$, and becomes turbulent for $Re_{\delta} > 1800$ (Fig. 4 shows only the laminar region). The liquid film thickness at the end of the laminar region is usually very small (≈ 0.1 mm). Heat convection correlations for the wavy and the turbulent regime exists (see e.g. Çengel-2003). All these correlations can be applied to slightly tilted plates by reducing gravity accordingly (i.e. by using $g \cos \theta$, but only if the wet surface faces upwards, as in natural convection in non-condensing fluids).

It was also Nusselt in 1916 who proposed a correlation for condensation on the outer surface of a horizontal cylinder, in the form $Nu_D = 0.725 Ra_D^{*1/4}$ (also applicable to a sphere by changing the coefficient to 0.815). Condensation in vertical cylinders can be studied as if vertical plates. It can be deduced that for cylinder slenderness $L/D > 3$, condensation is more effective in the horizontal configuration. Condensation in a horizontal tube bank is not as efficient as in single tubes (efficiency decreases roughly as the forth root of the number of tubes in a vertical row). For condensation in the inner surface of a tube, the vertical-plate model can be applied to vertical tubes, and the correlation $Nu_D = 0.56 Ra_D^{*1/4}$ to horizontal tubes when the entrance Reynolds number for the gas phase is $Re > 35\,000$. Table 1 gives a summary.

Table 1. Summary of natural heat convection correlations for film condensation (Ra^* is defined by (8) changing L to D).

Configuration	Correlation
Vertical plate	$Nu_L = 0.94 Ra_L^{*1/4}$
Vertical cylinder outside	$Nu_D = 0.94 Ra_D^{*1/4}$
Vertical cylinder inside	$Nu_D = 0.94 Ra_D^{*1/4}$

Horizontal cylinder outside	$Nu_D=0.73Ra_D^{*1/4}$
Horizontal cylinder inside	$Nu_D=0.56Ra_D^{*1/4}$
Sphere	$Nu_D=0.82Ra_D^{*1/4}$

Other correlations have been developed for several geometries, but the previous ones are the most important. Notice that the liquid layer would thermally-isolate the wall if not moving, as in condensation over a horizontal cold plate, and even worst if the condensate freezes (but this is no longer convection). Typical values of the heat-convection coefficient are in the range $h = \dot{q}/\Delta T = 10^3 \dots 10^4 \text{ W}/(\text{m}^2 \cdot \text{K})$.

Forced flow condensation

When a pumped flow of vapour comes in contact with a cold solid surface, liquid condensate appears if wall-temperature is below liquid-vapour-equilibrium temperature at the corresponding pressure. Forced flows of main interest in condensation are the flow over a flat plate, along a pipe, or external to cylinders (isolated or in tube banks), and in any case the two extreme geometries, vertical and horizontal, must be distinguished, since it is gravity in all cases what makes the condensate to pour. For instance, for forced pipe-flow along at moderate speed, where the condensate pours down the walls to the bottom (this stratified flow usually applies up to $Re_D < 35\,000$ based on the entrance conditions of the vapour), $Nu_D=0.56Ra_L^{*1/4}$ is often used. Typical values of the heat-convection coefficient are in the range $h = \dot{q}/\Delta T = 10^4 \dots 10^5 \text{ W}/(\text{m}^2 \cdot \text{K})$.

All the correlations above may be applied to mixtures, although the presence of a non-condensable gas decreases the heat-transfer rate, due to the diffusion-resistance it opposes.

TWO-PHASE LOOPS

Many heat-convection applications work in a steady state transferring heat from a source to a sink. Although this combined process might in principle be performed by solid conduction or by heat convection using a single-phase fluid, the most powerful means is by convection with phase change, i.e. by boiling a liquid at the heat source, transporting the vapour, and condensing it at the heat sink, returning the liquid to initial conditions and closing the cycle. The unavoidable pressure-loss in the circuit can be balance in several ways:

- Active pumping, usually by means of a hydraulic pump, since pumping the vapour is much less efficient. This mechanical pump is externally driven by an electric motor.
- Passive pumping (i.e. without applying external power), either taking advantage of buoyancy forces in a force field (thermosiphons), or taking advantage of capillary forces (heat pipes and vapour chambers). Another development makes use of the asymmetric flow of liquid slugs (between vapour plugs) in a temperature gradient, in what is known as pulsated heat pipe (PHP, see below), which works without recourse to gravity or capillary pumping in a porous media).

The most used pumped two-phase loop is the water/steam system at $p > p_{\text{amb}}$, working at $T > 100 \text{ }^\circ\text{C}$, used in heavy industries and district heating. Ammonia, alcohols, or halogenated hydrocarbons, have been used for lower working temperatures (e.g. R21 in the Shuttle and NH_3 in the ISS). Notice how far superior a

two-phase loop is compared with a single-phase loop: typical liquid-to-vapour phase-change absorbs about 1 MJ/kg (h_{LV}), whereas a liquid would had to be heated some 10^3 K to absorb the same energy (e.g. for water at about 50 °C, $h_{LV}=2.4 \cdot 10^6$ J/kg, $c=4200$ J/(kg·K), and hence $\Delta T=h_{LV}/c=2400/4.2=570$ °C).

Thermosiphons usually work by buoyancy in the gravity field, but they can be driven by centrifugal forces (e.g. in turbomachinery) instead of gravity. Contrary to heat pipes, thermosiphons do not require phase change of the working fluid. They are most used in solar heating, mainly without phase changes. In the latter case, the pumping pressure obtained by the difference in weight between the heated liquid column (of height L) and the colder one, with a temperature difference ΔT is $\Delta p=\Delta\rho gL=\alpha\Delta T\rho gL$; e.g. for $L=2$ m of water column with a $\Delta T=50$ °C, $\Delta p=0.3 \cdot 10^{-3} \cdot 50 \cdot 1000 \cdot 9.8 \cdot 2=300$ Pa, where a thermal expansion value of $\alpha=0.3 \cdot 10^{-3}$ 1/K (at 30 °C). Assuming laminar flow along a $L=10$ m circuit of a $D=10$ mm pipe, the obtained mass flow rate is $\dot{m}=\pi D^4 \rho \Delta p / (128 \mu L)=\pi \cdot (10^{-2})^4 \cdot 1000 \cdot 300 / (128 \cdot 10^{-3} \cdot 10)=7 \cdot 10^{-3}$ kg/s (26 L/h), corresponding to a solar gain of $\dot{Q}=\dot{m}c\Delta T=7 \cdot 10^{-3} \cdot 4200 \cdot 50=1.5$ kW.

In any case (active or passive pumping), the steady working of a cooling loop with phase change, can be represented in the p - T phase diagram by two LVE points in the $p_v(T)$ curve, say (p_E, T_E) for the boiling (traditionally named evaporation) and (p_C, T_C) for the condensation, but in the case of the liquid pump (and the thermosiphon) the driving $\Delta p=p_E-p_C$ is applied in the liquid phase at T_C , whereas in the case of a heat pipe it is applied as an underpressure at T_E . Pressure drop by flow friction is the same in all cases: the largest part is in the vapour line, followed by pressure drop in the liquid (particularly through the wick in heat pipes).

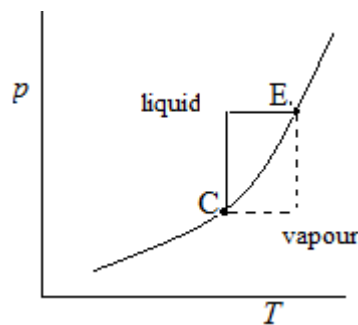


Fig. 5. Phase diagram of a cooling loop with boiling at E (evaporator) and condensation at C. The driving pressure in a mechanically-pumped loop is applied at point C (pressurising the liquid and then heating it to E), whereas in a heat loop the driving pressure is applied at E by capillary suction of the metastable liquid flowing through the wick interstices.

Heat pipes

A [heat pipe](#) (HP, Fr. *caloduc*, Sp. *caloducto*) is a passive heat connector consisting of a closed pipe, evacuated (air removed) and partially filled with liquid, which operates in an evaporation–condensation cycle, with vapour flow caused by a vapour-pressure gradient, and liquid flow due to capillary pumping in wicks or grooves. Internally, heat pipes are two-phase fluid-loops with phase change, self-pumped by capillary pressure (helped or hindered by natural convection in a gravity field), with fluid motion created in ultimate terms by the applied temperature difference between two zones of the device, as in natural convection.

Two main HP-types can be distinguished:

- Traditional, or simple, or stick heat pipe (SHP, Fig. 6a), with a straight or bent linear shape, and cylindrical or planar cross-section. The SHP consists of an evacuated metal tube closed at both ends, partially filled with liquid, and with some porous media all along the lateral inner wall, usually a wick, although grooves or simply the edges of non-smooth-cross-section ducts may work (the latter is used on micro heat pipes). The evaporator and condenser zones can be anywhere, even with more heating/cooling regions (e.g. the heat input in a middle region and two condensing regions at the ends). A variant of the SHP is the vapour chamber cooler, which is basically a planar two-dimensional heat pipe formed by two parallel plates (say $0.1 \times 0.1 \text{ m}^2$), with some internal wick layers or grooves (say 1 mm thick) enclosing a thin vapour space (say another 1 mm thick); heat input through a small region at one side, causes local boiling there, and condensation at all other colder areas; the liquid return is by spaced wicked struts.
- Loop heat pipe (LHP, Fig. 6b), with a circuit geometry, i.e. with the fluid moving in just one direction along a looping tube (with separate vapour and liquid pipes, not in crossflow as in the SHP). A LHP must have a compensation chamber (CC) to hold some spare liquid in contact with the wick (to keep it always wetted), and to allow a mass swing in the piping during operation. When the compensation chamber is not thermally-connected and integrated with the evaporator, and is located in the liquid line far from the evaporator, the device is known as a capillary pumped loop (CPL).

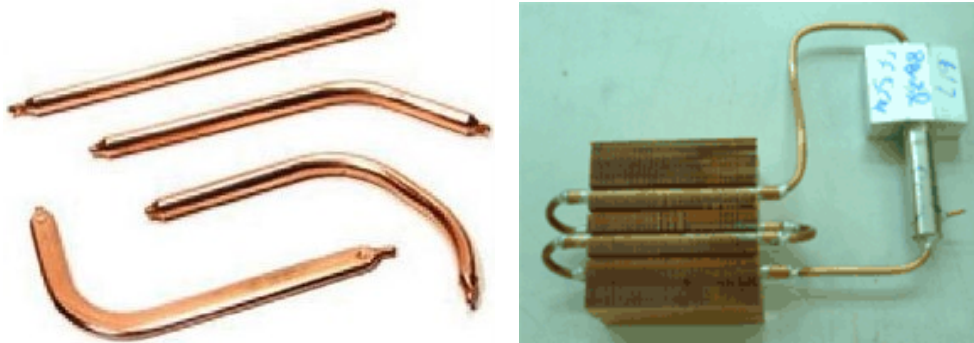


Fig. 6. a) Four traditional or stick heat pipe (SHP); the evaporator and condenser zones can be anywhere.
b) Loop heat pipe (LHP), with fins at the condenser zone; the evaporator is the white hand-written piece, and the compensation chamber is the metal bright adjacent element. (China-heatpipe.net).

Heat input to a HP must necessarily be at the wick element (the evaporator), but the condenser may be wicked, as in SHP, or not, as in LHP; in the latter, the condenser can be far away from the evaporator (up to several tens of meters in a horizontal position) because the vapour and liquid lines are smooth and flow resistance smaller.

From the outside, it is difficult to discern a SHP from a solid rod or bar, heat pipes being passive devices with opaque walls (copper most of the times), and similarly for a LHP, if not for the hissing of the fluid flow inside (usually water), and the difference in bulk density. The internal workings is sketched in Fig. 7.

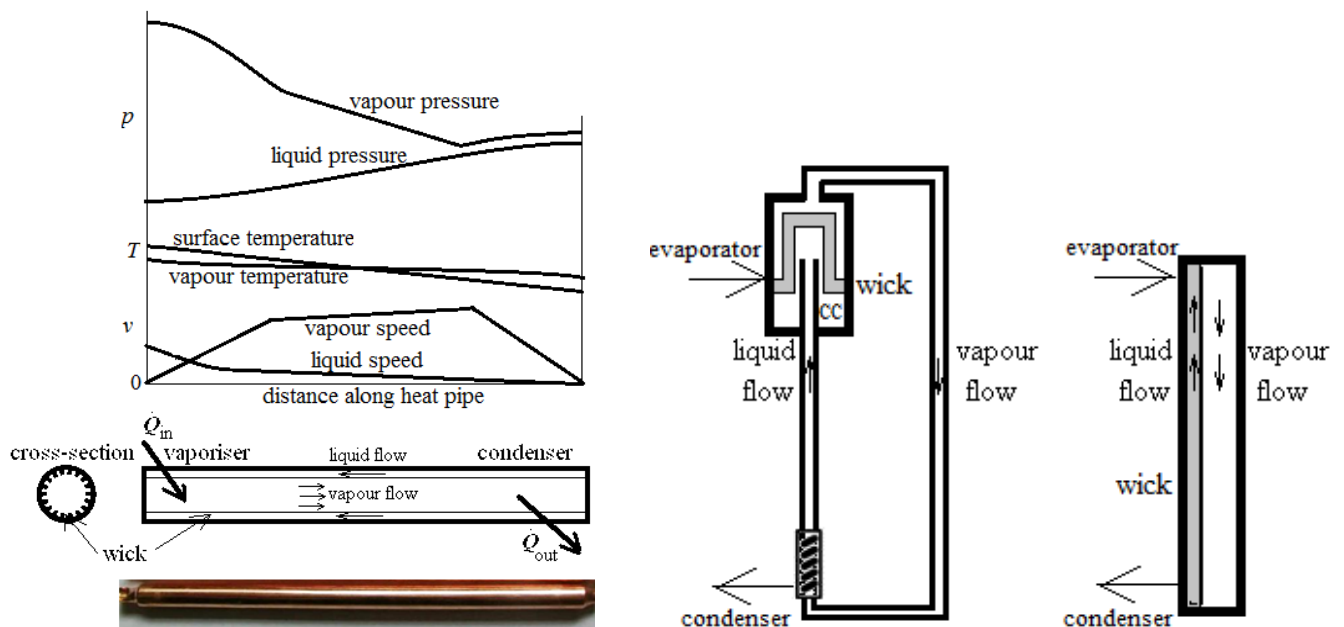


Fig. 7. a) A stick heat pipe (SHP), with sketches for internals, and pressure and velocity profiles during operation. b) Sketch of a loop heat pipe (LHP), and comparison with a SHP (in a planar 2D sketch), depicted as in a vertical position against the gravity field (adverse layout).

History and applications

Heat pipes were developed as an enhancement to thermosiphons; first introducing a two-phase flow on traditional liquid thermosiphons, and finally an grooved wall, allowing thermosiphons to work against gravity. First patent dates back to 1942, by R.S. Gaugler at General Motors, but first theoretical analysis dates from 1964, by George Grover, often referred to as the inventor of the heat pipe (he was the first to use the term "heat pipe" in his patent of 1963, at Los Alamos National Laboratory).

The technology was soon developed for space applications (high heat transfer rates with no moving parts); the first space trial was in 1967, for the thermal coupling between opposite surfaces of a non-rotating satellite (to avoid overheating of the sunlit one and undercooling on the shadowed one, both extremes causing malfunction of electronic systems). First time of HP use in a laptop was in 1994, and since then, they are widely used in consumer electronics, where copper is the preferred wall material, and water the most used working fluid.

At the beginning, heat pipes were just 'hollow copper rods', i.e. a sealed copper tube, partially filled with water or ammonia under vacuum, with grooves or a wick all along the inside surface (Fig. 7a). Heat is transferred from one end region to the other end region by internal convection of a fluid undergoing a phase change, instead of by simple conduction as in a copper rod. Modern developments in heat pipe technology tend to use LHP, to reduce the wicked section to just the evaporator (where the capillary pumping takes place), reducing flow resistance through it, completing the circuit with smooth piping for the vapour and liquid lines (and the condenser). The first LHP was built in 1972 by Gerasimov and Maydanik (Ural Polytechnical Institute, Sverdlovsk, USSR), having a length of 1.2 m and a capacity of about 1 kW, with water as a working fluid. The first patent is of 1985, and the first spacecraft use was in 1994. LHP are currently the baseline thermal connectors used in deployable radiators.

In the SHP design (Fig. 7a), variations in liquid volume during transients are accommodated within the longitudinal wick extending all along the HP, but in the LHP a dedicated compensation chamber (CC) must be provided (since the amount of liquid soaking the wick is not enough), usually integrated with the evaporator as depicted in Figs. 6b and 7b.

A different HP design is the so-called pulsating heat pipe (PHP), initiated by Akachi in 1990. It has a circuit layout like the LHP, made of a large capillary tube (say 4 mm internal diameter on normal gravity, much larger possible under microgravity), bended in several turns, alternated in contact with the heat source and the heat sink. When filled with the fluid like in any HP, the liquid forms capillary plugs, separated by vapour spaces in a random manner. When connected to the heat source and sink in a steady way (without imposing any heat-flux changes), an unsteady periodic pulsation develops in the fluid inside because vapour plugs expand at the hot bends and contract at cold bends, and the initial random asymmetry gets amplified until a coherent motion develops in just one direction (unknown beforehand). Most promising are thin flat evaporators made of smaller fluid channels, e.g. 0.5 mm deep channels (a few millimetre wide) milled in a 1 mm thick plate, and covered with a 0.5 mm thick plate.

A HP is usually the best cooling solution to get rid of powers from 1 W to 1 kW from heat sources to heat sinks at moderate distances, say 0.1 m to 10 m. For smaller powers or shorter distances, heat conduction through a metal element may be better, and for larger powers or longer distances, forced heat convection is better (best with two-phase flow), while thermal-radiation heat-transfer dominates at higher temperatures (or when the environmental fluid does not help, as in [spacecraft thermal control](#)). In comparison with metal conduction (e.g. $k_{\text{copper}}=390 \text{ W}/(\text{m}\cdot\text{K})$), a HP usually has $k_{\text{eff}}\gg 1000 \text{ W}/(\text{m}\cdot\text{K})$, and in comparison with forced convection (e.g. $h_{\text{water}}\approx 500 \text{ W}/(\text{m}^2\cdot\text{K})$), a HP usually has $h\gg 1000 \text{ W}/(\text{m}^2\cdot\text{K})$. The key to these high-conductance characteristics of heat pipes lays in the vaporisation enthalpy (of order $10^6 \text{ J}/\text{kg}$, equivalent to a liquid heating of about one thousand degrees!), and the associated small temperature-drop between evaporator and condenser (it is directly related the difference in vapour pressure, which cannot be high for proper HP working). Notice, however, that HP should not be modelled as a solid bar of very high conductivity, because thermal resistance, $R\equiv\dot{Q}/\Delta T=L/(kA)$, is almost independent on L in heat pipes, and the working geometry is different (contact points for hot and cold sides are not the two end-bases of a rod SHP, but a larger lateral area at the evaporator, and a much larger area at the condenser).

Heat pipes are highly efficient passive heat-transfer devices: they have lower mass and lower volume than equivalent heat conductors, and are used to evacuate heat from internal parts of spacecraft, [computers](#), lighting systems (e.g. above 500 W for outdoor flood leds, about 200 W for leds in large indoor spaces), medical diagnostics (e.g. cooling endoscope heads), [constructions on permafrost](#) (to efficiently evacuate from the ground to colder air, the heat received from the supported system through its foundations, as in the Alaska pipeline, where 122 000 ammonia-in-mild-steel heat-pipes were installed), and so on. Heat pipes are usually independent items to be connected to the source and sink, but they might be machined

on the substrate itself of an electronic device (e.g. making grooves by etching the underside of an epitaxially-grown circuit on the other side).

Operations overview

The workings of a heat pipe is difficult to predict because of the interplay between thermo-physical and fluid-dynamic processes. The level of detail and effort demanded greatly varies from a conceptual description to the quantitative design. An overview of the sequential stages in HP utilisation and design may be:

- Concept (fundamentals). The key component of a HP is the pumping element, i.e. the porous media (usually a wick) which forces the flow and compensates the pressure loss due to fluid flow resistance inside the whole HP. A HP does not require gravity to work, but gravity may limit (or favour) HP performance. The fluid inside is in liquid-vapour equilibrium; hence a HP may work at any temperature between the triple point and the critical point of the working fluid (though interfacial and transport properties greatly reduce this range). Under isothermal conditions, vapour pressure inside a HP is uniform and related to temperature by Clapeyron's equation, $p=p_v(T)$, whereas pressure in the liquid may be uniform but distinct (because of the menisci), or even have an hydrostatic profile (in a gravity field); in the latter case, the meniscus radius will change with height to accommodate the uniform vapour pressure. The high internal pressure at high temperature, $p_v(T)$, favours a cylindrical geometry for the HP for strength, but there is a tendency nowadays towards rectangular elements (planar HP) at least in the main heat-transfer elements (evaporator and condenser) to avoid the saddle-shape fixture needed to have good thermal contact with a planar heat source.
- Operation (principles). When heat is applied over the soaked wick (cooling may work the same in a SHP, but not on a LHP), vapour is generated to rise pressure locally ($p_v(T)$), and the high-pressure vapour pushes itself along the vapour line towards a heat exchanger where it condenses (because there is ample contact with colder surfaces; the surface area of the vapour line is relatively small). The condensate is pushed along the liquid line back towards the porous matrix in the evaporator, where a positive pressure-jump takes place by capillarity at the hot menisci, closing the fluid cycle. Heat pipes profit from self-regulation, in the sense that if higher thermal loads are imposed, the evaporator gets hotter, vapour pressure increases, and fluid flow increases, promoting higher heat transfer rates, trying to cope with the imposed increase (within limits).
 - The operating temperature of a HP is defined as that of evaporation, $T_E \approx T_{\text{source}}$, and depends on heat-power input (the higher \dot{Q} , the higher T_E), and heat-sink temperature (which may be 5..50 °C lower). Notice that the condensation temperature cannot be too-much smaller than the evaporation temperature, since capillary pressure-jump in a HP is small (typically around 5 kPa), and Clapeyron's equation shows that $dp/dT|_{\text{sat}}$ is rather large, e.g. for water at 50 °C, $dp/dT|_{\text{sat}}=0.6$ kPa/K, so that for $\Delta p=5$ kPa, $\Delta T=5/0.6=8$ K (and even smaller for other working fluids: $dp/dT|_{\text{sat}}=50$ kPa/K for NH₃ at 50 °C, so that for $\Delta p=5$ kPa, $\Delta T=5/50=0.1$ K).
 - The heat power transmitted by a HP is defined at the evaporator, but can be either computed by measuring heat input to the evaporator (usually using an electrical resistor insulated outwards), or by measuring the heat input from the condenser to the heat sink

(usually a single-phase fluid loop, since there is usually no need to take into account heat transfer to the environment from the vapour and liquid lines, although the temperature changes might be large (e.g. in the liquid line of a LHP, temperature at the evaporator entrance may be 20..40 °C larger than at the condenser exit, and still the heat-gain be small, $c\Delta T/h_{LV} \ll 1$).

- Specific HP characteristic are usually referred to evaporator surface, A_E , but in some cases to the vapour-line cross-section, A_V . As for temperature drop, there is little difference to use the evaporator surface temperature or the evaporation temperature, T_E , but the other temperature should be the condensing temperature, T_C , because temperature in the condenser varies a lot, both in the HP fluid (between entrance and exit), and in the cooling medium.
 - HP heat flux is defined by $\dot{q} \equiv \dot{Q}_E/A_E$; e.g. 5 W/cm² for a typical 8 mm diameter 0.2 m long water-in-copper HP.
 - HP conductance is defined by $G \equiv \dot{Q}_E/(T_E - T_C)$, and thermal resistance by $R=1/G$.
 - HP conductance coefficient is often defined by $K_E \equiv (\dot{Q}_E/A_E)/(T_E - T_C)$, often named convective coefficient with symbol h ; e.g. 5 W/(cm²·K) for a typical 8 mm diameter 0.2 m long water-in-copper HP, with 5 cm long evaporator. However, sometimes an ‘axial’ conductance is defined, in terms of the vapour-line cross-section, A_V (both for SHP and LHP), by $K_V \equiv (\dot{Q}_E/A_V)/(T_E - T_C)$, with corresponding higher values (e.g. 100 W/(cm²·K) for the same device).
- Modelling (mathematics). To a first approximation, for a heat pipe in steady operation, $\dot{Q}_{in} = \dot{Q}_{out} = \dot{m}h_{LV}$, but it is difficult to predict the mass flow rate, \dot{m} , which depends on the forcing pressure, $\Delta p_C \approx 2\sigma/r \approx p_V(T_E) - p_V(T_C)$. Once the geometry and inventory (mass of fluid) known, the governing equations to be solved may be as follows:
 - Thermodynamic relations. For the whole, close system, the global energy balance is $dE/dt = \dot{Q}_{in} - \dot{Q}_{out}$; for each internally-opened element, the local energy balance is $dE/dt = \dot{Q}_{in} - \dot{Q}_{out} + \dot{m}_{in}h_{in} - \dot{m}_{out}h_{out}$; liquid-vapour equilibrium (Clapeyron’s equation), $dp_V/dT|_{sat} = h_{LV}/(Tv_{LV})$, gives $p_V(T)$.
 - Heat-transfer relations: conduction heat transfer in the solid parts (e.g. $\dot{Q} = kA\Delta T/\delta$ for a planar wall of thickness δ), and thermal convection correlations at fluid surfaces (i.e. a Nussel-number correlation and $\dot{Q} = hA\Delta T$ with $h=kNu/D$).
 - Fluid-flow relations: to model the pressure-drop by friction at every element (usually in the form $\Delta p = \frac{1}{2}c_K\rho v^2$). In SHP the largest pressure drop is in the liquid return through the wick, due to the much smaller open cross-section area through the porous media, whereas in LHP it is in the vapour line, due to the much higher speed (for similar liquid and vapour line diameters). The capillary pumping takes place at the evaporator in all cases, and is $p_V - p_L = 2\sigma \cos\theta / r$, where σ is the liquid surface tension (of the order of 10⁻² N/m), θ the liquid contact angle (smaller than 90° for liquids on metals), and r the meniscus radius (of the order of 10⁻⁶..10⁻⁴ m, a fraction of pore size d of the wick; e.g. $r=0.2d$).
- Performances (characteristics). To select a HP from the market offer, one must be aware of several criteria, knowing that HP performances are dictated by gravity orientation, besides manufacturing

details: working fluid (and residual non-condensing gases, if any), materials, and geometrical details (pipe diameters, bending, flattening, junctions).

- Working temperature range. It is delimited by the available heat-sink temperature and the maximum tolerable source temperature. This T-range almost defines the type of working fluid: most HP work at around room temperature, but heat pipes have been developed to work at cryogenic temperatures (e.g. nitrogen in stainless steel HP), or at very high temperatures (e.g. sodium in stainless steel HP working at 1000 K, or silver in a tantalum HP working at 2000 K).
- Cooling power range. It delimits the HP-size and wick type. As said above, HP are self-regulated (the more heat-power applied at the evaporator, the more flow-rate developed and the more heat power evacuated at the condenser); to a first approximation, cooling power and evaporator temperature are proportional; e.g. for a 1 cm diameter water-in-copper HP, $\dot{Q}=G(T_E-T_C)$ with $G=20..40$ W/K (thermal resistance $R=1/G=0.02..0.05$ K//W). External control, to limit the heat flow, may be achieved by modifying the thermal conductance at the condenser side; e.g. in the classical HP, variable conductance was achieved by letting some additional non-condensing gas inside, N₂ or Ar; other way is by changing the active area of the condenser.
- Geometry (heat-path length and cross-section). It defines the effective thermal conductivity needed, i.e. $k_{\text{eff}} \equiv \dot{Q}L/A$, which is >1000 W/(m·K) in small HP and can approach 100 000 W/(m·K) in long loop heat pipes, in comparison with 390 W/(m·K) for copper. HP-geometry must match the location and size of the heat source and heat sink. Distance and gravitational orientation must be within suitable bounds; otherwise, solid conductors for short lengths, or pumped fluid loops for longer lengths may be needed.
- As an example, consider a typical Cu-H₂O heat-pipe for laptop-CPU-cooling, having $D=8$ mm in diameter and 0.2 m long (5 cm evaporator, 10 cm adiabatic, 5 cm condenser), with a heat load of $\dot{Q}=50$ W when the temperature drop is $T_E-T_C=1$ °C. If the evaporator area is $A_E=\pi DL_E=13$ cm², the heat flux is $\dot{Q}/A=50/(13 \cdot 10^{-4})=40\,000$ W/m² (4 W/cm²), and the convection coefficient at the evaporator is $h=\dot{Q}/(A\Delta T)=50/(13 \cdot 10^{-4} \cdot 1)=40\,000$ W/(m²·K)=4 W/(cm²·K). An axial convection coefficient can be defined in terms of the external cross-section $A=\pi D^2/4$ (but using just the vapour flow cross-section allows a common definition for SHP and LHP); $h=\dot{Q}/(A\Delta T)=50/(0.5 \cdot 10^{-4} \cdot 1)=100$ W/(cm²·K). An effective axial conductivity can be defined too, with the external cross-section or the vapour cross-section, and with the adiabatic length; in our example, $A=0.5$ cm², $L=0.1$ m, and $k_{\text{eff}} \equiv \dot{Q}L/A=50 \cdot 0.1/(0.5 \cdot 10^{-4})=100\,000$ W/(m·K).
- Design (project). Requirements on temperature, power, size, working fluid, material of the wick, container material, geometry, etc. From initial specifications, to manufacturing and tests.
 - Evaporator design (this is the key element of a HP). High heat flux requires:
 - Working fluids with liquid-vapour transition at the desired working temperature, T_E , with high vaporization enthalpy, h_{LV} , high surface tension, σ , and good wetting (small contact angle, θ , to wick material).

- For a SHP (Fig. 7a), $m_{\text{tot}}=m_{\text{wick}}+m_{\text{core}}$, where m_{wick} is the mass of fluid within the wick (or grooves), either in liquid or in vapour phase, and m_{core} is the mass of fluid outside the wick or grooves (just vapour if no liquid entrainment occurs).
- For a LHP (Fig. 7b), $m_{\text{tot}}=m_{\text{cc}}+m_{\text{wick}}+m_{\text{v,grooves}}+m_{\text{v,line}}+m_{\text{cond}}+m_{\text{l,line}}$. The compensation chamber usually includes a bayonet tube that guarantees that the wick is always wet at the central core.

Several different heat-pipe configurations enable additional capabilities, as heat-flow regulation (variable conductance heat pipe, VCHP), diode performance (when the wick is only at one end, heat can only be transmitted away from it to the other end), mechanically flexible heat pipes, etc. Heat-pipe conductance can be controlled passively (e.g. adding some inert gas that gets trapped at the condenser with a temperature-dependent inert volume, or an internal thermostatic valve, as in VCHP), or actively (e.g. externally changing the inert-gas temperature, or externally changing the position of an internal valve, or heating the compensation chamber in a CPL). In some applications, the cooled instrument requires the operation temperature to be maintained within a very narrow range, what can be accomplished within certain limitations by actively controlling the compensation chamber saturation temperature (with a resistor, or with a thermoelectric device), but the overall conductance degrades.

Current trends in HP development are on high-performance wicks, miniaturization, cheap manufacturing, nanofluids... Nanofluids are common fluids seeded with nanometric particles which may highly increase thermal conductivity and wettability (e.g. water with 1 % by mass of copper particles of size $d=10..100$ nm, increases k from $0.6 \text{ W}/(\text{m}\cdot\text{K})$ for pure water to $1 \text{ W}/(\text{m}\cdot\text{K})$, and lower the water-copper contact angle from 66° to 25° , what increases capillary pumping and retards wick dry-out.

Design and operating limits

A heat pipe has many constraints that must be taken into account for proper design and operation, among which:

- Capillary limit. Heat pipes rely on the pressure jump created in the menisci of a liquid-vapour interface in the wick, which on wick of porous size d (which we may approximate as a bundle of capillary tubes of diameter d , or a little bit small; think of the interstices between the tubes), is limited by the Young-Laplace law to $\Delta p=4\sigma/d$ (assuming perfect wetting), which, for typical values of surface tension ($\sigma=10^{-2} \text{ N}/\text{m}$) and porous sizes ($d=10^{-5} \text{ m}$) yields $\Delta p=4\cdot 10^{-2}/10^{-5}=4 \text{ kPa}$, a rather small pumping power (capable of rising water to a maximum of 0.4 m). This is the only available pumping pressure to overcome all pressure losses due to friction in the vapour line, condenser piping, liquid line, and evaporator (including the high pressure loss of the liquid across the wick), the adverse hydrostatic load (if any), and the small capillary counter-pressure at the vapour-liquid interface in the condense (capillary jump at the liquid-vapour interface in the compensation chamber is always negligible).
- Gravity limit. Heat pipes can only work for distances typically smaller than 1 m in adverse elevation. An adverse elevation (or adverse tilt) means that the evaporator is above the compensation chamber in a gravity field. A heat pipe cannot work with a high adverse elevation because of the hydrostatic load, $\Delta p=\rho_l g z$, added to the circulation friction-load; e.g. a 1 m water

column imposes a $\Delta p = 1000 \cdot 9.8 \cdot 1 = 9.8$ kPa, and the only available capillary pumping gives $\Delta p < 2\sigma/r$; for water in a wick of $d = 10$ μm (particle size, say $r = 0.2d$ for porous radius), the pumping, $\Delta p < 2 \cdot 0.07 / (2 \cdot 10^{-6}) = 7$ kPa < 9.8 kPa, is not sufficient. One might think that using nanometric-size wicks can enlarge at will this gravity bound; e.g. if the porous radius is $r = 10$ nm, the pumping power might reach $\Delta p = 2\sigma/r = 2 \cdot 0.07 / 10^{-8} = 14$ MPa, i.e. 140 m of water column, and in fact we have a good example in the [pumping of sap-tree from root to top](#) (almost 100 m high in the giant sequoias). Increasing adverse tilt increases evaporator temperature, T_E (because Δp must be higher).

- Bounds in filling fluid mass, m_{\min} and m_{\max} . If there is insufficient liquid, the wick might become dry, stopping fluid flow. If there is too much liquid, the LP may explode when heated. Typical filling ratios are 50..75 % by volume.
- Bounds in storage temperature, T_{\min} and T_{\max} . If the liquid freezes inside, the wick may be spoiled, and the HP crack, in the case of water. If the temperature is too high, the liquid may expand to completely fill the remaining vapour space, and the container may yield by the pressure surge (a HP is a pressure vessel and must be designed accordingly). In a LHP, the total fluid volume (empty volume before filling) is $V_{\text{tot}} = V_e + V_{\text{vl}} + V_c + V_{\text{ll}}$, where V_e is evaporator empty volume, V_{vl} vapour-line volume, V_c condenser volume, and V_{ll} liquid-line volume. The evaporator empty volume is $V_e = V_{\text{cc}} + \phi_{\text{pw}}V_{\text{pw}} + \phi_{\text{sw}}V_{\text{sw}} + V_g$, i.e. comprises that of the compensation chamber + primary wick (porosity times bulk volume) + secondary wick + vapour groves. The total mass of working fluid is limited to $m_{\text{tot}} = \rho_{L, T_{\max}} V_{\text{tot}}$.
- Bounds on applicable heat power, \dot{Q} , and associated operating temperature (that of the evaporator, T_E). There is a threshold to start the HP (to initiate fluid motion): the minimum heat-power input to initiate nucleate boiling inside the evaporator wick, particularly if it is completely filled with liquid. With sufficient heating, both SHP and LHP will self-start operating (CPL needs priming but has a quicker start than the LHP), but the start-up may be slow at low heat-rates (e.g. 2..20 min for motion to start, the larger for the smallest heat loads). In LHP, just after start-up, oscillations in compensation temperature can be large (temperature overshoots).
 - At low T_E (really, near the lower end of the operation temperature range), especially at start-ups, pressure jump in the vapour line may be too large (the pressure at the condenser end of the pipe can be very small), restricting the vapour flow. If this restriction is just by viscosity, transmitted heat power will be limited to $\dot{Q}_{\text{viscous-limit}} = D_V^4 h_{LV} \rho_V (p_E - p_C) / (64 \mu_V L_V)$, where D_V is the diameter of the vapour line, and all vapour properties are computed at T_E . If the restriction is due to sonic choking, transmitted heat power will be limited to $\dot{Q}_{\text{sonic-limit}} = 0.34 \cdot D_V^2 h_{LV} \sqrt{\rho_V (p_E - p_C)}$.
 - At moderate T_E (really mid operating range) and high heat loads \dot{Q} , vapour velocity may be sufficiently high to produce shear-force effects on the liquid at the wick surface, particularly in SHP. The limit heat-power to avoid this liquid entrainment is $\dot{Q}_{\text{entrain-limit}} = D_V^2 h_{LV} \sqrt{\sigma \rho_V / d}$, where d is the pore diameter of the wick.
 - At very high heat-loads, the wick at the evaporator can become dry, because, as \dot{Q} increases, the transversal ΔT across the wick increases, exceeding the degree of superheat sustainable in relation to nucleate boiling conditions, causing the onset of boiling within

the wick, and the downstream propagation of the boiling front, eventually leading to "dry out" and liquid circulation stop. This boiling limit is due to excessive transversal heat flux; all the other limits are due to axial heat flux. In practice, only capillary limit and boiling limit must be considered. An estimate of the maximum heat flux for a planar wick of thickness δ and effective thermal conductivity $k_{\text{eff}} = \phi k_L + (1-\phi)k_S$ (parallel heat-path through solid matrix and liquid filling) is:

$$\dot{q} = k_{\text{eff}} \frac{T_E - T_C}{\delta} \frac{\Delta p_{\text{nucl}} - \Delta p_{\text{capil}}}{\rho_V h_{LV}} \quad (11)$$

where $\Delta p_{\text{nucl}} = 2\sigma/r_{\text{nucl}}$ is the nucleation pressure jump (corresponding to a typical nucleation radius of $r_{\text{nucl}} = 10^{-6}$ m), and $\Delta p_{\text{capil}} = 2\sigma/r$ is the capillary pressure (corresponding to a meniscus of radius r).

- Maximum temperature difference between evaporator and compensation chamber in a LHP. As the capillary pressure pumping, Δp_C , is limited by wick details, and pressure and temperature are linked by Clapeyron's equation, the temperature jump is limited to $\Delta T = \Delta p_C / (dp/dT)_{\text{sat}}$; for instance, for an ammonia LHP with a maximum capillary jump of 5 kPa, and ammonia LVE data at 15 °C, the temperature jump from the compensation chamber to the generated vapour $\Delta T_{\text{cc,e}} = \Delta p_C / (dp/dT)_{\text{sat}} = (5 \text{ kPa}) / (25 \text{ kPa/K}) = 0.2 \text{ K}$ (but for water at 50 °C, $\Delta T_{\text{cc,e}} = \Delta p_C / (dp/dT)_{\text{sat}} = (5 \text{ kPa}) / (0.6 \text{ kPa/K}) = 8 \text{ K}$).

In some applications, notably in the cooling of mobile electronic devices, HP operation is limited by overall heat-sink conductance (final heat convection to ambient air, usually forced with a fan), and not by any internal HP limit.

Thermodynamic processes in a LHP

A piecewise model can be used to describe HP operation, with 4 major components: the evaporator (always wicked, and including the compensation chamber in a LHP), the condenser, the vapour line, and the liquid line. The workings of a HP is best explained with the aid of the p - T diagram of the change of phase in pure substances, as shown in Fig. 8, briefly explained as follows: vapour generated in the evaporator goes along the vapour line from 1 to 2 (i.e. losing pressure by friction, but maintaining its temperature because global heat transfer from gas to gas is very small); vapour enters the condenser at state 2 and leaves it at state 3 (i.e. it cools, condenses, and subcools, losing pressure by friction along the way); the liquid condensate loses pressure along the liquid line from 3 to 4, enters the evaporator at state 4 (which may approach state 5' by heat gains from the evaporator), moves from 5' to 5 in metastable liquid state through the wick, and has the capillary pressure jump from 5 to 1 at the evaporating meniscus.

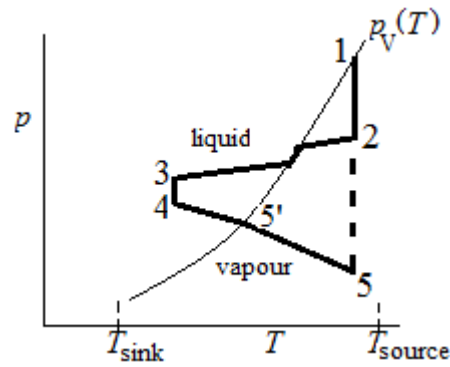


Fig. 8. Sequential processes in a heat pipe: 1-2 vapour line, 2-3 condenser, 3-4 liquid line, 4-5-1 evaporator.

The detailed explanation of Fig. 8 is as follows. Consider a heat pipe (e.g. water in copper, either SHP or LHP) working at steady state:

- State 1. This is the liquid-vapour equilibrium in the vaporisation interface (considered planar; in the highly-curved wick menisci, the vapour is at state 1 but the liquid in the other side of the meniscus is at metastable-state 5). Due to finite axial extent of the vaporisation interface, state 1 with the highest pressure in the system will occur at the far downstream point, and another state 1', slightly down of point 1 in Fig. 8, will better represent the condition of the vapour exiting the evaporator and entering the vapour line (in a LHP, 1' is a little bit hotter than 1 because vapour in the external grooves of the wick is closer to the heat source than the meniscus downwards, the hottest being the outer wall, and there is some viscous pressure drop from 1 to 1'). In a SHP, vaporisation takes place at the internal radius of the wick, in spite that the external radius is hotter, because of the absence of nucleation sites in the latter.
- Process 1 to 2. The relatively high pressure vapour at 1 flows along the vapour line to the entry of the condenser at 2, with high viscous pressure drop because of the high speed associated to a low density in a constant mass-flow-rate, $\dot{m} = \rho v A$), maintaining its temperature if insulated (or with a small T-drop to the environment, if not). In a LHP, the vapour being generated goes towards the vapour line and not in the opposite sense through the wick because the former flow-path has less flow-resistance.
- Process 2 to 3. This is the heat evacuation (to a colder heat sink) at the condenser, with a first part of vapour cooling, a middle part of two-phase cooling (initially with a film condensation at the wall, growing inwards until the last vapour bubble condenses), and a last part of liquid cooling.
- Process 3 to 4. This is the liquid return line, a separate pipe in a LHP, with a small viscous pressure drop, and all along the wick in a SHP, with a larger pressure drop, (Fig. 7). In principle, wall heat transfer from 3 to 4 is small even without external insulation, but the small flow rates and the metallic joint at the hot evaporator may cause the entry point 4 to actually be near point 5' in Fig. 8, which in a LHP corresponds to the liquid-vapour equilibrium inside the compensation chamber.
- Process 4-5'-5-1. All this takes place inside the evaporator element (comprising the compensation chamber in a LHP). As just said, the entrance may be anyway between points 4 and 5' in Fig. 8. In fact, for a LHP, point 5' corresponds to the steady mixing of the colder liquid return flow with the standing liquid inside the compensation chamber, with heat input by conduction from the heat

source by two heat paths: through the wick, and through the joining container wall, known as back-conduction heat losses (Fig. 7b).

- The process 5' to 5 seems to be in the vapour region in Fig. 8, but it is actually the flow of liquid through the wick, which cannot transform to vapour because of the absence of nucleation points in a well-wetted porous media of micrometre pore size. The liquid gets superheated but boiling is prevented by the strong liquid cohesion in such reduced dimensions, until a free surface at point 5 facilitates the boiling.
- The process 5 to 6 is not really a process but an abrupt jump through the meniscus interface (of monoatomic thickness), from the low-pressure convex liquid side to the high-pressure concave vapour side, of value $\Delta p = 2\sigma \cos\theta/r$, where σ is the interface tension, θ the contact angle (small in most cases), and r the radius of the spherical cap best adjusting the meniscus apex (a hemisphere for $\theta=0$ at rest).

Notice that the general decreasing of surface tension σ of pure working fluids with increasing temperature ($\sigma=0$ at the critical point, with the maximum value at the triple point; the simplest correlation was already proposed by van der Waals: $\sigma = \sigma_{tr}(1-T/T_{cr})$) is detrimental to heat pipe operation. There are, however, some mixtures that show a positive slope in $\sigma(T)$ in some temperature range (e.g. dilute aqueous solutions of butanol or higher alcohols).

Table 2. Some typical HP working fluids and HP performances.

Working temperature [°C]	Working fluid	Surface tension ² σ [N/m]	Container material	Maximum heat flux \dot{q}_E [W/cm ²]
-190..-80	Nitrogen (N ₂)	0.012 at -160 °C	SS ¹	1
-70..90	Ammonia (NH ₃) ³	0.022 at 15 °C	SS, Ni, Al	10
-50..150	Methanol (CH ₃ OH)	0.020 at 50 °C	Cu,Ni,SS	50
5..250	Water (H ₂ O) ⁴	0.072 at 50 °C	Cu,Ni	100
400..900	Potassium (K), or sodium (Na)	0.12 at 750 °C	Ni, SS	150
900..1500	Li	0.26 at 1250 °C	Nb with 1 % Zr	200
1500..2000	Ag	0.80 at 1700 °C	Ta with 5 % W	400

¹SS=stainless steel. ²Temperature dependence can be approximated linearly to $\sigma=0$ at the fluid critical point. ³Ammonia should not be used with copper. ⁴Water in copper is most used in HP for electronics cooling (in the range 40..140 °C).

Flow inside the wick

Wick structure may be categorized by:

- Gross uniformity: homogeneous (monopore), or composite (a two layer compound wick, one highly conducting with small pores, and the other highly insulating with coarse pores, is the best).
- Fine uniformity: coherent (like grooves), or stochastic (like sintered powders).
- Construction method: a) sintered powder metal, b) wire mesh (wrapped screen mesh), c) grooves, or d) fibre/spring. Coherent wicks made by hole-etching on silicon wafers are also used, for research.

Grooved walls are the simplest wick to manufacture (and the first used), but the least efficient (limited to about 5 W/cm^2), and cannot work against gravity. Most modern wicks are made of sintered metal powder because they have the highest capillary pumping pressure, and best heat transfer flux (about 50 W/cm^2 , up to 250 W/cm^2), but they are expensive to manufacture and integrate (sometimes they are sintered in situ, i.e. directly inside the container). Most used sintered wicks are made of copper, nickel, or titanium, with typical porous radius $r=1..10 \text{ }\mu\text{m}$, porosity $\phi=55..75\%$, permeability $\kappa=(0.1..2)\cdot 10^{-12} \text{ m}^2$, and effective conductivity $k_{\text{Cu,wick}}=20..40 \text{ W/(m}\cdot\text{K)}$, $k_{\text{Ni,wick}}=5..10 \text{ W/(m}\cdot\text{K)}$, $k_{\text{Ti,wick}}=1..2 \text{ W/(m}\cdot\text{K)}$.

Aiming at a better understanding of this crucial aspect of heat pipe theory, a deeper analysis on porous media parameters (pore-size and porosity), and flow characterization, both steady (permeability), and transient (sorptivity), is worth pursuing.

Wicks are [porous media](#), i.e. a continuous pore space (void space, usually a single contiguous fluid-fillable medium, but multiple unconnected tubes in some special wicks), surrounded by a continuous solid phase called the matrix (to have mechanical strength; we do not consider loose solid material). By convention in fluid-flow studies, the definition of pore space excludes any void pocket that is totally enclosed within the solid material. By extension, a single capillary tube can be included as a porous media. We consider only fix solid geometry (i.e. indeformable). Example of porous media: a bunch of thin tubes (say $<1 \text{ mm}$ in diameter), a bunch of parallel ‘hairs’ (like in a brush), a twisted bunch of fibres, paper, wood, a sugar cube, a sponge (either of the fibre type, or of foamed polymers), a clay brick, compacted powders (e.g. soils), sintered powders, rocks (though porosity of metamorphic rocks may be negligible in comparison with sedimentary rocks)...

Parameters of porous medium:

- Mean pore size, d . This parameter seems simple to understand, but it is difficult to define with precision (and hence to measure it) in most real porous media (except perhaps in 2D geometries). But precision is seldom needed, and it is often understood as a typical equivalent diameter of porous in a 2D cut of the material (i.e. a circle of the same area), or even approximated as the typical diameter of the particles used in a forming the medium (if made of particles), since the ratio of particle diameter to pore diameter is $V_{\text{solid}}/V_{\text{void}}=(1-\phi)/\phi$ which is of order unity (e.g. for equal spheres, the Cartesian arrangement has $(1-\phi)/\phi=(1-0.476)/0.476=1.1$, and maximum packing yields $(1-\phi)/\phi=(1-0.26)/0.26=2.8$). Notice that the mean porous size is not representative of the wettable surface-area because of the poor [sphericity](#) of voids, most of the times concave. For equal mean-size of particles, porosity decreases when size-range increases (small particles tend to occupy voids between larger-particles). For same-size particles, porosity does not depends on size; e.g. for equal spheres in the most compact arrangement, porosity is $\phi=0.26$ for cannon balls and for carbon atoms in diamond; notice, however, that porous media analysis requires $L \gg d$ (there is no point in considering three grains of sand and the space between them as a porous medium), and that we only envisage here porous media flow as a continuum (i.e. when molecular flow has a mean free path $\lambda \ll d$).

- **Porosity**, ϕ . This is the void fraction, i.e. volume of fillable voids over the total volume (matrix and voids); $\phi \equiv V_{\text{void}}/V_{\text{total}} = 1 - \rho_{\text{bulk}}/\rho_{\text{solid}}$ (the last equality deduced from the total-mass relation: $m_{\text{total}} = m_{\text{solid}} = \rho_{\text{solid}}V_{\text{solid}} = \rho_{\text{bulk}}V_{\text{total}}$, and $V_{\text{void}} = V_{\text{total}} - V_{\text{solid}}$; notice the difference between solid (or particle) density, $\rho_{\text{solid}} \equiv m_{\text{solid}}/V_{\text{solid}}$, and bulk density, $\rho_{\text{bulk}} \equiv m_{\text{solid}}/(V_{\text{solid}} + V_{\text{void}})$. Porosity can be measured by densitometry, by volumetry (with a wetting liquid), by differential weighting of a soaked and a dried sample, by gas expansion to an evacuated sample, by optical methods (in a representative surface, or by tomography). Particle density can be measured by Archimedes' principle. For porous media formed by [regularly arranged spheres](#) of the same diameter, porosity is $\phi = 0.476$ for a Cartesian arrangement, $\phi = 0.320$ for a body-centred cubic arrangement (bcc), and $\phi = 0.260$ for the most-compact packing (there are several arrangements with this porosity: face-centred cubic, hexagonal, and one version of tetrahedral bcc); spheres randomly thrown together will have $\phi = 0.30..0.35$ (the effect of non-spherical shape is not important, but porosity decreases if several sizes are mixed up). For a [pack of circular rods](#), porosity is $\phi = 0.215$ in a square arrangement, and $\phi = 0.093$ in the most-compact hexagonal case. Porosity of typical clay bricks is about $\phi = 0.25$. Related to porosity (void fraction) is void ratio, $V_r \equiv V_{\text{void}}/V_{\text{solid}} = \phi/(1-\phi)$, i.e. $\phi = V_r/(1+V_r)$. Recall that the pore network must be a continuum (no closed pores are accounted). Notice also that some people use ϕ for heat flux [W/m²] and ε for porosity. Porosity quickly decreases when sintering or firing powders at high temperature.

Parameters of porous medium flow:

- Number of fluid phases. It may be one or several liquid phases (e.g. water+oil), and/or one gas phase. Each phase may have its fixed or changing composition (according to the interaction between the fluids and the matrix: solving, absorbing, or reacting).
- Volume fraction, α , of one fluid-phase in the whole void volume (porosity is void volume fraction). Considering all phases, $\sum \alpha_i = 1$ (and still $\phi < 1$). When fluids are not pure chemical species, and concentration specification is required, the same notation as used in [Mixtures](#) (where the fluid occupied the whole volume, i.e. $\phi = 1$) applies. Notice that bulk properties of a porous medium containing some fluids, depend on relative proportions; e.g. the effective thermal conductivity of a wick depends on the conductivities of solid, liquid, and vapour, and on their relative amounts: $k_{\text{eff}} = (1-\phi)k_s + \phi(\alpha_L k_L + \alpha_V k_V)$.
- **Permeability**, κ , is the coefficient for flow-rate in a porous media according to Darcy's law (1856), $\dot{V}/A \equiv v_A = -(\kappa/\mu)\nabla p$, stating that, for a single fluid flow in a porous media, the volume flow-rate, \dot{V} , per unit cross-section area, A , named Darcy speed, v_A , is directly proportional to the forcing (total pressure gradient along the flow, $\nabla p = \Delta p/L$), and inversely proportional to fluid viscosity, μ ($\mu = \rho\nu$) with a coefficient κ [m²] (non-SI unit is the darcy: 1 darcy $\approx 10^{-12}$ m²) named permeability, κ , which is dependent basically on pore size d , and to a lesser extent on porosity, ϕ , but almost the same for liquids and gases. Notice that Darcy speed, v_A (also named gross filtration speed, or [superficial velocity](#)) is smaller than the mean velocity through the pore channels; this pore or interstitial speed v_i , is $v_i = v_A/\phi$, where ϕ is the porosity (void fraction). In any case, flow inside porous media is at very low Reynolds number ($Re = v_i d/\nu \ll 1$) and therefore laminar.

The driving forces may be: gravity ($\nabla p = -\rho g$), buoyancy ($\nabla p = -\Delta \rho g$), applied pressure (∇p), or capillary pressure ($\nabla p = -\Delta p_c/L = -2\sigma \cos\theta/(rL)$, where r is the pore radius, θ the contact angle, and L the friction length).

The dependence of permeability on pore size and porosity, $\kappa = \kappa(d, \phi)$, may be deduced by applying Poiseuille law (fully developed laminar flow) to a capillary tube of radius R (the mean porous radius), what yields the average speed, $v = (R^2/(8\mu))\nabla p$; identifying the latter with Darcy law, we find $\kappa = R^2/8 = d^2/32$, with d being the mean pore size (diameter). But, for a wick of pore size d (say square channels), area of cross-flow A , and porosity ϕ , the number of pore channels is $A\phi^{2/3}/d^2$, so that, in terms of the diameter of the particles D ($D/d = (1-\phi)/\phi$), a much used $\kappa(D, \phi)$ -relation is the [Kozeny–Carman equation](#) (1927):

$$\kappa = \frac{\phi^3}{180 \cdot (1-\phi)^2} D^2 \quad (12)$$

though the empirical non-dimensional coefficient 180 is sometimes chosen as 150. A typical fine-mesh sintered-Cu wick may have a mean particle diameter of $D = 10 \mu\text{m}$, a thickness about $t = 100 \mu\text{m}$, porosity about $\phi = 0.6$, and permeability about $\kappa = 10^{-12} \text{ m}^2$ (from (12), $\kappa = 0.6^3 \cdot (10 \cdot 10^{-6})^2 / (180 \cdot (1-0.6)^2) = 0.3 \cdot 10^{-12} \text{ m}^2$). Notice that, for a given particle size, actual pore size depends on sintering pressure and temperature.

The relation between flow rate and pressure gradient in a porous media (Darcy's law) becomes:

$$\frac{\dot{V}}{A} \equiv v_A = \frac{\kappa}{\mu} \nabla p = \frac{\phi^3 d^2}{180 \mu (1-\phi)^2} \nabla p \quad \left(\text{or} \quad \nabla p = \frac{180 \mu (1-\phi)^2}{\phi^3 d^2 \Phi^2} v_A \right) \quad (13)$$

where the [sphericity](#) factor $\Phi \equiv A_{sp}/A_p$ (area of an spherical particle with the same volume, divided by true area of the particle) has been added in the last form in (13). Another such a relation is [Ergun equation](#) (1952):

$$\nabla p = \frac{150 \mu (1-\phi)^2}{\phi^3 d^2} v_A + \frac{1.75 \rho (1-\phi)}{\phi^3 d} v_A^2 \quad (14)$$

The pressure drop can also be set in the common fluid-dynamic way (with $\nabla p = \Delta p/L$) as:

$$\Delta p = \lambda \frac{L}{d} \frac{1}{2} \rho v_A^2 \quad \text{with} \quad \lambda = \frac{360 \cdot (1-\phi)^2}{\phi^3 \Phi^2 Re} \quad \text{or} \quad \lambda = \frac{300 \cdot (1-\phi)^2}{\phi^3 Re} + \frac{3.5 \cdot (1-\phi)}{\phi^3} \quad (15)$$

where Reynolds number is based on Darcy speed v_A and mean particle diameter d , i.e. $Re = v_A d / \nu$. Recall that in the case of fully-developed laminar flow in pipes, it is $\lambda = 64/Re$ in (15), with Reynolds number

based now on mean viscous speed (half the central speed in a circular pipe) and pipe diameter. Porous flows with $Re < 10$ may be considered laminar, and Darcy's law applied.

In the case of radial flow (cylindrical geometry), Darcy's law $\dot{V}/A \equiv v_A = -(\kappa/\mu)\nabla p$ must be multiplied by the changing area to get the pressure drop explicit, i.e. as the volumetric flow-rate, \dot{V} , is constant in any case (at the steady state):

$$\frac{\dot{V}}{A} \equiv v_A = \frac{\kappa}{\mu} \nabla p \rightarrow \dot{V} = A \frac{\kappa}{\mu} \nabla p \begin{cases} \dot{V}^{\text{planar}} = A \frac{\kappa}{\mu} \frac{dp}{dx} = A \frac{\kappa}{\mu} \frac{\Delta p}{L} \\ \dot{V}^{\text{cylin}} = 2\pi r W \frac{\kappa}{\mu} \frac{dp}{dr} = 2\pi W \frac{\kappa}{\mu} \frac{dp}{d \ln r} = 2\pi W \frac{\kappa}{\mu} \frac{\Delta p}{\ln \frac{r_{\text{ext}}}{r_{\text{int}}}} \end{cases} \quad (16)$$

where W is the width of the cylindrical porous media, and r_{int} and r_{ext} the limiting radii. In other way:

$$\Delta p_{\text{cylin}} = \frac{\dot{V} \mu}{2\pi W \kappa} \ln \frac{r_{\text{ext}}}{r_{\text{int}}} \quad \left(\Delta p_{\text{planar}} = \frac{\dot{V} \mu L}{A \kappa} \right) \quad (17)$$

Parameters of transient flow in porous medium:

- [Sorptivity](#), S [$\text{m/s}^{-1/2}$], is the capacity of the medium to absorb or desorb liquid by capillarity, as introduced in 1957 by John Philip. Liquid suction at the base of a porous material in horizontal flow (for powder particles, a tube closed by a wide-pore filter at the bottom is filled), is modelled as:

$$\frac{\dot{V}}{A} \equiv v_A \equiv \frac{S}{2\sqrt{t}} \leftrightarrow x_{\text{wet}}(t) = \frac{V}{A} = S\sqrt{t} \quad (18)$$

stating that the gross infiltration speed v_A (Darcy speed) decays with time as $t^{-1/2}$ (there is a singularity at $t=0$), or, equivalently, that the wet front $x_{\text{wet}}(t)$ advances along the porous media with time in a way proportional to $t^{1/2}$. Notice that the volumetric flow rate, \dot{V} [m^3/s], does not coincide with the change in wet volume per unit of time, dV/dt ; porosity helps to find the relation: $\dot{V} = \phi dV/dt$. Sorptivity depends on materials porosity (void fraction). Sorptivity of typical clay bricks is about $5 \text{ mm} \cdot \text{min}^{-1/2}$. Within the range of useful porous sizes, sorptivity is almost inversely proportional to porosity, and sometimes sorptivity is defined as to include this effect, i.e. as $S\phi$ (almost a constant in that range); fortunately, the range of useful porosities is not great, e.g. $\phi=0.4..0.8$, so the order of magnitude is the same. Sorptivity can be easily measured by plotting the advancing wet front distance versus time and applying (18). The simplest analytical formulation is the [Washburn's equation](#) (1921) describing capillary flow in a cylindrical tube in absence of gravity effects (but applies to imbibition into porous materials, if an effective tube diameter is appropriately chosen):

$$x_{\text{wet}}(t) = \sqrt{\frac{\sigma d \cos \theta}{4\mu} t} \rightarrow S = \sqrt{\frac{\sigma d \cos \theta}{4\mu}} \quad (19)$$

Sorptivity measurements can be used to find the advancing contact angle (if all other parameters are known) by plotting $x_{\text{wet}}^2(t) = \sigma d \cos \theta t / (4\mu)$. For vertical capillary rise, Xue-2006 deduced:

$$\frac{\rho g}{6\sigma \cos \theta} x_{\text{wet}}^3 + \frac{x_{\text{wet}}^2}{d} = \frac{\sigma \cos \theta}{4\mu} t \quad (20)$$

Boiling inside the wick

The boiling at the wick (which is rather thin) may show different details; e.g. in the traditional SHP (Fig. 7a), the vapour–liquid interface is near the inner edge of the wick, whereas in the LHP (Fig. 1b) the vapour–liquid interface is close to the outer edge of the wick.

To simplify the model, consider a regular structured 2D wick composed of circular wires separated a small distance (say, up to one diameter apart), fully soaked in liquid, as sketched in Fig. 9.

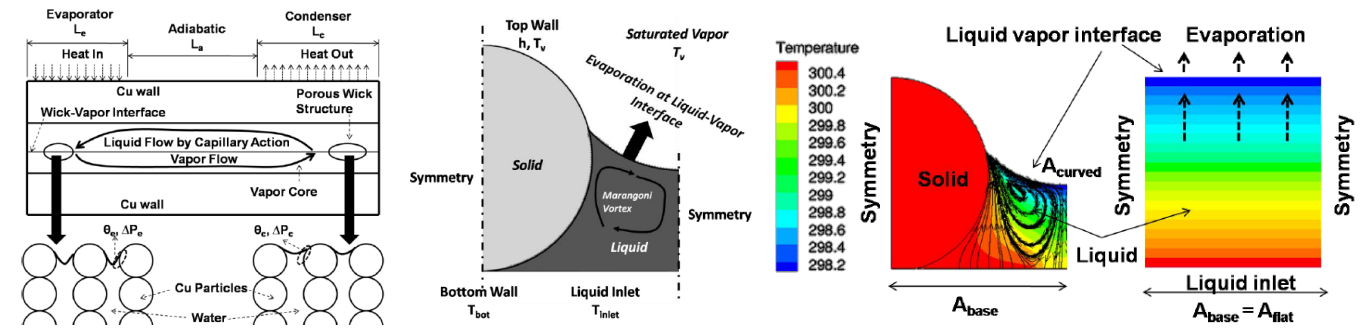


Fig. 9. a) Sketch of menisci in a flat HP. b) Detail with Marangoni cell. c) Temperature profiles and streamlines for $T_{L,in}=300.5$ K and $T_v=298$ K, in the meniscus, and in a 2D interface (2010-Ranjan).

Micrometre-size menisci in thermodynamic equilibrium are spherical patches, but, in a temperature gradient with the solid-wall hotter than the liquid, they show more elongated shapes, with three zones:

- A very-thin-film region (a few nanometres thick) creeping on the hot solid and non-evaporating because of the strong adhesion (disjoining pressure); it is isothermal.
- A transient region where most of the gradients and the vaporisation take place, with Marangoni flow in the liquid.
- A small central quasi-spherical meniscus region, where vaporisation is less important because of the smaller ∇T .

The effect on equilibrium vapour pressure due to the millimetric size inside the porous wick is described by Langmuir's law (a linear expansion of Kelvin's equation). For a concave liquid surface with radius of curvature r , vapour pressure becomes:

- Kelvin's equation: $p_v(T,r) = p_v(T) \exp[\Delta p_c / (\rho_L R T)] = p_v(T) [1 - \Delta p_c / (\rho_L R T)] = p_v(T) - \Delta p_c \rho_v / \rho_L$.
- Langmuir's law: $p_v(T,r) = p_v(T) - \Delta p_c \rho_v / (\rho_L - \rho_v)$.

where $p_v(T,r)$ is the vapour pressure (depending on temperature and curvature radius, with $\Delta p_c = 2\sigma/r = p_v - p_L$ for concave voids, $p_v(T)$ is the vapour pressure in a planar surface, ρ_L and ρ_V are the liquid and vapour densities, and $R = R_u/M$ the gas constant ($R_u = 8.3 \text{ J}/(\text{mol}\cdot\text{K})$ and M its molar mass).

The effective curvature radius, r , for the meniscus formed by a wetting liquid in packed uniform spheres of diameter d is $r = 0.21 \cdot d$ (Chi-1976).

The boiling within a wick does not always take place at the wick border, and several different configurations may be reached depending on the heating power applied (see Fig. 10a). In a typical LHP-geometry, the liquid-vapour interface may recede as sketched in Fig. 10b, where a fully soaked wick between two grooved copper plates is subjected to a large temperature difference.

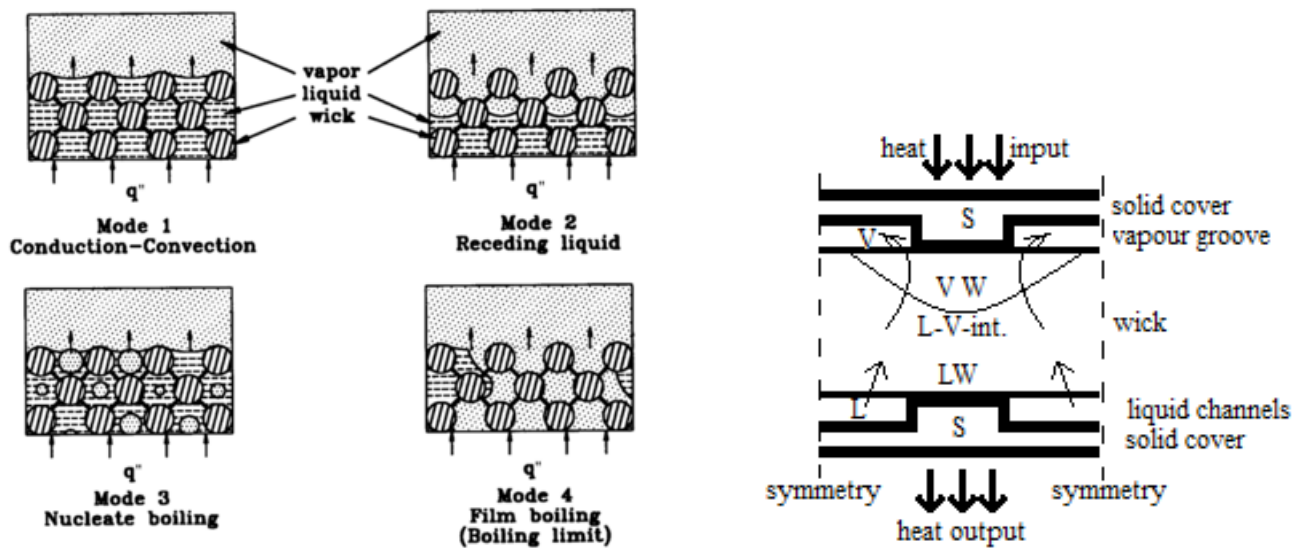


Fig. 10. a) Four modes of nucleate boiling in a wick (Faghri, 1995). b) Detail of a planar evaporator contour in a mini LHP, showing the liquid-vapour interface inside the wick: L, liquid input; L-V, liquid-vapour interface; VW, vapour-filled wick; V, vapour out; S, solid wall.

EVAPORATIVE COOLING

Evaporative cooling is the thermal effect associated to a solutal relaxation process involving a phase change, i.e. the thermal-energy loss that balances the vaporisation energy, $h_{LV} \dot{m}_w / A_{wet}$, due to the mass-flow-rate of a volatile species (usually water) at the interface.

Although it applies to any substance, the most common case of evaporative cooling concerns water evaporation in air because, most of the times, the vapours are discarded (what would be uneconomical and unecological, otherwise). The cooling effect of evaporating water can be large in dry climates, and evaporative cooling is increasingly used in [air conditioning](#); it can even be used even for [ice making](#).

Evaporation in a pool of water

If a pool of water is in contact with air, and there is a gradient in chemical potential of water, i.e. the air is not saturated, some liquid will evaporate at the interface (evaporation is an interface phenomena, whereas boiling is more a bulk phenomenon). The vaporisation enthalpy gained by the liquid passing to vapour,

produces a refrigeration effect because that energy is extracted either from the liquid (because of its larger conductivity), or from the gas (if the liquid mass is small and already cooled).

If all the heat comes from the air side (good approximation for small water masses at quasi-steady state), the cooling effect can be estimated by balancing the heat-rate per unit area, $h\Delta T$, convected (or conducted across the boundary-layer thickness δ), with the required vaporisation energy, $h_{LV} \dot{m}_w / A_{wet}$:

$$\dot{q} = h\Delta T = k \frac{\Delta T}{\delta} = h_{LV} \dot{m}_w / A_{wet} = h_{LV} \rho_a D_i \frac{\Delta W}{\delta} \Rightarrow \Delta T = \frac{h_{LV} \rho_a D_i}{k} \Delta W = \frac{h_{LV}}{c_{pa} Le} \Delta W \quad (21)$$

where the mass flow-rate has been approximated by Fick's law across the boundary-layer thickness, and w is humidity ratio (absolute humidity). The diffusivity of water-vapour in air at room temperature and pressure is $D_i=22 \cdot 10^{-6} \text{ m}^2/\text{s}$, changing proportionally to $T^{3/2}/p$. The result is that the difference between air and water temperature (dry bulb minus wet bulb) is practically equal to the difference for the adiabatic saturation process, $c_{pa}\Delta T + h_{LV}\Delta W = \text{constant}$, analysed in the [Thermodynamics of humid air](#) (since $Le \approx 1$; already implied in the assumption of equal δ).

Evaporative cooling is limited by mass diffusion. For instance, if one thinks on how long it would take for a cup of water to evaporate in vacuum (e.g. opening the cup's lid in outer space), the answer is that, first, the whole water mass would quickly cool from the boiling at the initial temperature and its corresponding vapour pressure, until the freezing is attained at about 273 K and 0.6 kPa (the triple point of water), greatly reducing further losses; from that on, the sublimation rate would be the same as the effusion from the equilibrating gas (same temperature and vapour pressure), i.e. some $(1/6)n\nu$, n being the amount of gas per unit volume, $n=p/(RT)=611/(8.3 \cdot 273)=0.26 \text{ mol}/\text{m}^3$, and $\nu=(3kT/m)^{-1/2}=400 \text{ m/s}$, i.e. $(1/6)0.26 \cdot 400=17 \text{ mol}/(\text{s} \cdot \text{m}^2)$. And the temperature would continue to decrease by evaporative cooling of the ice, decreasing the sublimation rate.

The rate of evaporation in a pool of water in ambient air, quiescent or windy, is an important engineering and environmental problem that has deserved thorough analysis. It was Dalton in 1801, after introducing the partial pressure concept, who first stated that the evaporation rate is proportional to the difference in partial pressure of water vapour from the saturated boundary layer, $p^*(T_w)$, to that of the air far aside, $\phi p^*(T_a)$, and that it increases with free air velocity. Carrier in 1918 proposed a correlation for the evaporative flux in the form:

$$\dot{m}_w / A_{wet} = (c_1 + c_2 v_a) [p^*(T_w) - \phi p^*(T_a)] / h_{LV}, \quad \text{with } c_1 = 0.09 \text{ m/s and } c_2 = 0.07 \quad (22)$$

e.g., for water at $T_w=25 \text{ }^\circ\text{C}$ and a mild air stream at 3 m/s, $T_a=30 \text{ }^\circ\text{C}$ and 50 % RH, the evaporation rate is $\dot{m}_w / A_{wet} = (0.09 + 0.07 \cdot 3)(3170 - 0.5 \cdot 4250) / (2.4 \cdot 10^6) = 130 \cdot 10^{-6} \text{ (kg/s)/m}^2 = 130 \cdot 10^{-9} \text{ m/s} = 15 \cdot 10^{-3} \text{ m/day}$, i.e. some 15 mm of water level drop per day. Notice that a faint breeze with a wind speed of $v_a=1.5 \text{ m/s}$ doubles the evaporating rate (that is why swimming pools should have wind barriers to save water).

However, in a similar way as when giving precipitation data in height of water collected instead of litres per square metre, it seems more convenient to state evaporation rates in terms of receding-velocity of the water surface, v_{evap} (typically a few mm/day) instead of in terms of mass-flow-rate per unit area, $\dot{m}_w / A_{\text{wet}}$ (e.g. in (kg/s)/m²). Their relation, and the definition of boundary-layer thickness mentioned above, δ , as well as that of the empirical mass-transfer-coefficients in terms of absolute humidity, $h_{m,w}$, and of relative humidity, $h_{m,\phi}$, is:

$$v_{\text{evap}} = \frac{\dot{m}_w / A_{\text{wet}}}{\rho_w} \stackrel{\dot{m}=\rho v A=\text{const.}}{=} v_v \frac{\rho_a}{\rho_w} \stackrel{\text{Fick's law}}{=} \frac{D_i \nabla \rho_v}{\rho_w} = \frac{\rho_a}{\rho_w} D_i \nabla y_v = \frac{\rho_a}{\rho_w} D_i \frac{\Delta w}{\delta} = \frac{1}{\rho_w} h_{m,w} \Delta w = \frac{1}{\rho_w} h_{m,\phi} \Delta \phi \quad (23)$$

where v_v is the diffusion velocity of the vapour in the air, continuity at the interface means $\rho_w v_{\text{evap}} = \rho_v v_v$, $\rho_v \approx y_v \rho_a$, $\rho_v = w \rho_a$, and Fick's law is $\dot{m}_w / A_{\text{wet}} = -D_i \nabla \rho_v$. Approximating [humidity ratio](#) as $w = M_{va} \phi p^*(T)/p$, where $M_{va} = M_v/M_a = 0.622$, the speed of water evaporation is:

$$v_{\text{evap}} = \frac{\rho_a}{\rho_w} D_i \frac{\Delta w}{\delta} = \frac{\rho_a}{\rho_w} D_i M_{va} \frac{\Delta(\phi p^*)}{\delta p} = \frac{\rho_a}{\rho_w} D_i M_{va} \frac{p^*(T_w) - \phi p^*(T_a)}{\delta p} \quad (24)$$

e.g., for a glass of water in air at 25 °C ($p^* = 3.17$ kPa), 100 kPa, and 50 % RH, assuming a 1 cm typical thickness of the diffusion layer (from water surface to ambient air), we have $v_{\text{evap}} = (1/1000) \cdot 22 \cdot 10^{-6} \cdot 0.622 \cdot (3.17 - 0.5 \cdot 3.17) / (0.01 \cdot 100) = 22 \cdot 10^{-9}$ m/s = 1.9 mm/day.

Carrier equation (22), rearranged in terms of receding velocity, becomes:

$$v_{\text{evap}} = (c_1 + c_2 v_a) \frac{p^*(T_w)}{p} \left(1 - \phi \frac{p^*(T_a)}{p^*(T_w)} \right), \quad \text{with } c_1 = 4 \cdot 10^{-6} \text{ m/s and } c_2 = 3 \cdot 10^{-6} \quad (25)$$

e.g., for the example above with a $v_a = 3$ m/s wind, $v_{\text{evap}} = (4 \cdot 10^{-6} + 3 \cdot 10^{-6} \cdot 3) \cdot 0.0317 \cdot (1 - 0.5 \cdot 4250/3179) = 136 \cdot 10^{-9}$ m/s = $16 \cdot 10^{-3}$ m/day. Uncertainties of ± 30 % should be expected in practice, due to specific boundary conditions in each particular case. The length of the boundary layer developed over the water pool also has an effect, though small (decreasing the evaporating rate up to a 20 % for more than 100 m surface length).

Ocean evaporation is a critical part of Earth's water cycle. Averaged over the whole surface of the sphere, the annual evaporation of the oceans is about 0.9 m/yr, balanced by an equal annual precipitation of 0.9 m/year globally (it rains more over the oceans, 1 m/yr, than over land, 0.7 m/yr; by the way, about 2/3 of that continental precipitation returns directly to the atmosphere by evapo-transpiration). Evaporation in the equatorial region, where raining is the heaviest, is less high than in the subtropical regions, where dry air from the Hadley cell falls down; evaporation (and precipitation) is minimal in polar regions, which are snow-covered only because the small accumulation of snow every year does not sublimates very much, not because it snows a lot there.

The evaporation of liquid droplets has also received great attention because of its applications to sprays, diesel injection, clouds, rain, etc. A generic correlation for the evaporation rate of a droplet (of any liquid) moving through air is:

$$Sh \equiv \frac{h_m D}{D_i} = 2 + 0.6 Re^{1/2} Sc^{1/3}, \quad \text{with} \quad \dot{m}_{\text{liq}} = h_m \pi D^2 (\rho_{v,s} - \rho_{v,\infty}) \quad (26)$$

valid for $2 < Re < 800$. Notice that the mass-transfer coefficient, h_m , can be assumed constant during the evaporation process, i.e. the quasi-steady state is with mass-flow-rate and area varying linearly with time (the squared diameter law already found by Langmuir); the dimensions of h_m in (26) are those of a velocity, and $Re \equiv v_a D / \nu_a$, and $Sc \equiv \nu_a / D_i$. The same type of correlation can be used to compute the convective coefficient, h :

$$Nu \equiv \frac{hD}{k} = 2 + 0.6 Re^{1/2} Pr^{1/3}, \quad \text{with} \quad \dot{Q} = h \pi D^2 (T_\infty - T_s) = \dot{m}_{\text{liq}} h_{LV} \quad (27)$$

Example 1. Find the evaporation time for a water droplet 1 mm in diameter when travelling at 10 m/s in air at 25 °C, 50 % RH and 100 kPa.

Solution. Assuming quasi-steady process, air data at these conditions are $\nu_a = \mu_a / \rho_a = 15 \cdot 10^{-6} \text{ m}^2/\text{s}$ (from [Gas Data](#)), $D_i = D_{\text{water vapour, air}} = 22 \cdot 10^{-6} \text{ m}^2/\text{s}$ (from [Diffusivity Data](#)), $Sc \equiv \nu_a / D_i = 15/22 = 0.70$, $Re \equiv v_a D / \nu_a = 10 \cdot 0.001 / (15 \cdot 10^{-6}) = 650$, and from (15) $Sh = 2 + 0.6 Re^{1/2} Sc^{1/3} = 15.6$, $h_m = Sh D_i / D = 0.34 \text{ m/s}$. Now, for humid air $\rho_v = w \rho_a$, with $\rho_a = 1.17 \text{ kg/m}^3$, w_s is the saturation humidity ratio for adiabatic humidification ($T_{\text{wet-bulb}} = 17.6 \text{ °C}$), $w_s = 0.013$ (13 g/kg), and w_∞ is the humidity ratio of ambient air, $w_\infty = 0.010$ (10 g/kg). Thence, for an initial area is $\pi D^2 = 3.14 \cdot 0.001^2 = 3.1 \cdot 10^{-6} \text{ m}^2$, the rate of evaporation is $\dot{m}_{\text{liq}} = h_m \pi D^2 \rho_a (w_s - w_\infty) = 0.34 \cdot 3.1 \cdot 10^{-6} \cdot 1.17 \cdot (0.013 - 0.010) = 3.7 \cdot 10^{-9} \text{ kg/s}$, which, for an initial mass of $\rho_w \pi D^3 / 6 = 1000 \cdot 3.14 \cdot 0.001^3 / 6 = 0.52 \cdot 10^{-6} \text{ kg}$, yields an evaporation time of $t_{\text{evap}} = 0.52 \cdot 10^{-6} / 3.7 \cdot 10^{-9} = 140 \text{ s}$.

If, instead of finding the mass-flow rate with (26), the heat-flow rate is found with (27), we have $Pr \equiv \mu_a c_{pa} / k_a = 18 \cdot 10^{-6} \cdot 1000 / 0.024 = 0.75$ (from [Gas Data](#)), $Nu = 2 + 0.6 Re^{1/2} Pr^{1/3} = 15.9$, $h = Nu k_a / D = 380 \text{ W}/(\text{m}^2 \cdot \text{K})$, $\dot{Q} = h \pi D^2 (T_\infty - T_s) = 380 \cdot 3.1 \cdot 10^{-6} \cdot (25 - 17.6) = 0.0088 \text{ W}$, and, from (27) $\dot{m}_{\text{liq}} = \dot{Q} / h_{LV} = 0.0088 / (2.4 \cdot 10^6) = 3.9 \cdot 10^{-9} \text{ kg/s}$, just the same result as by the previous method.

It can be further worked that, if the droplet had no relative speed to the air, it would stay for some 1100 s before dissolving in the quiescent air, whereas for dry air (at 10 m/s) the lifespan would reduce to some 60 s.

Notice that, contrary to problems of condensation and boiling, which involved cold or hot walls, evaporative cooling is driven by a liquid-vapour interface gradient, what can hugely increase the heat-transfer area if the interface is disperse, as in cooling towers. Evaporative cooling devices (for indoor and outdoor ambient control), and heat rejection devices (such as cooling towers), are commonly used to

provide significantly lower temperatures than those achievable with simple air cooling or dry heat-rejection devices.

Cooling towers

It is known that all industrial processes, as all living organisms, need to get rid of waste heat to be in a steady state (entropy generation must be balanced by entropy flow outwards). For airborne industries and living beings, the heat must flow to the surrounding air, but air is a thermal insulator, and, although blowing air enhances the transfer by one or two orders of magnitude, it is not enough in some circumstances, but Nature showed us an ultimate resource: sweating, a mild form of ablation (i.e. losing part of the body to protect the rest). The cooling tower (or wet tower), is a direct-contact heat-exchanger, a common industrial application of evaporative cooling.

A [cooling tower](#) is usually an intermediate device to get rid of heat from another system: a water stream cools the system (much more efficiently than air: four or five orders of magnitude more than still air), and then is finely dispersed over an upcoming stream of air; what causes some water evaporation and the consequent cooling of the remaining water (that must provide the vaporisation enthalpy).

The flow of water is always forced with a pump, and the flow of air usually forced with a fan, although in the largest cooling towers (those of large power stations) air is circulated by natural convection. Those huge cooling towers, able to transfer 1000 MW from water to air, are more than 100 m high and near 50 m in diameter, with a typical hyperboloid shape for maximum structural strength, not for thermal purposes. The tower is just an empty chimney, since the filling is only 3 m high and just above the ground-level air-openings, with 0.2 m thick walls made of steel-reinforced concrete; the main working load is its own weight, that with this shape results in stresses being transmitted down two diagonal straight-lines (hyperboloid construction) instead of just one (cylindrical construction). In those high chimneys, vertical variations of ambient temperature should be accounted for (± 5 °C typically, favourable during daytime and detrimental during night-time temperature inversion).

There are two basic types of cooling towers (Fig. 6), direct (or open), and indirect (or closed). In the simplest cooling tower, the water that is cooled by evaporation within the tower, is actually the coolant of the main system to cool. An indirect or closed cooling tower circulates the water through tubes located in the tower. In this type of tower, the cooling water does not come in contact with the outside air.

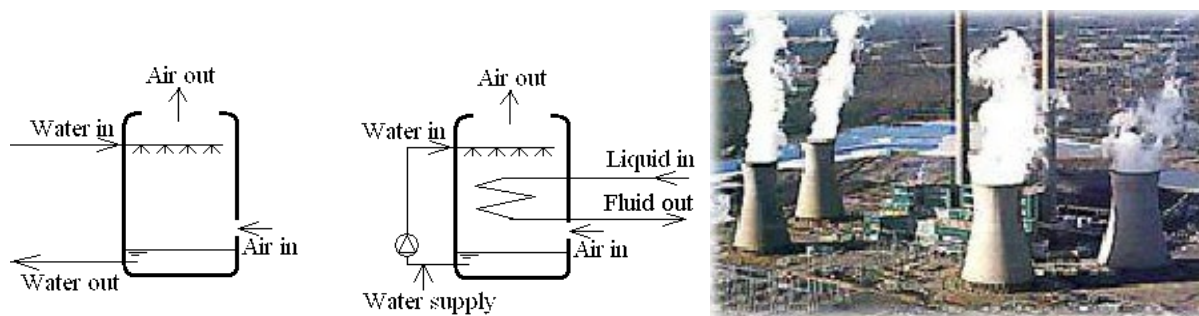


Fig. 6. Cooling towers: a) simple (or open, or direct), b) 'closed' or indirect, c) Photo of natural draft cooling towers in a 800 MW combined-cycle power-plant. Only the flows are indicated in the

sketches; other vital components, as the fan to force the air flow, the filling to enhance heat-and-mass transfer, and the drop scrubbers to minimise water losses, are not shown.

[Back to Heat transfer](#)

[Back to Thermodynamics](#)